UNCLASSIFIED

AD 427 130

DEFENSE DOCUMENTATION CENTER

FOR

SCIENTIFIC AND TECHNICAL INFORMATION

CAMERON STATION, ALEXANDRIA, VIRGINIA

UNCLASSIFIED

NOTICE: When government or other drawings, specifications or other data are used for any purpose other than in connection with a definitely related government procurement operation, the U. S. Government thereby incurs no responsibility, nor any obligation whatsoever; and the fact that the Government may have formulated, furnished, or in any way supplied the said drawings, specifications, or other data is not to be regarded by implication or otherwise as in any manner licensing the holder or any other person or corporation, or conveying any rights or permission to manufacture, use or sell any patented invention that may in any way be related thereto.

64-7

ASD-TDR-63-693

42 7 130

CATALOGED BY ASTIA AD No.

Application of Aerodynamic Lift in Accomplishing Orbital Plane Change

Roland N. Bell, 1/Lt, USAF
Wilbur L. Hankey, Jr., Ph.D.

TECHNICAL DOCUMENTARY REPORT NO. ASD-TDR-63-693

September 1963

427 130

presented at

JAN 20 1964

ASD 1963 Science and Engineering Symposium

Aeronautical Systems Division
Air Force Systems Command
Wright-Patterson Air Force Base, Ohio

NOTICES

When Government drawings, specifications, or other data are used for any purpose other than in connection with a definitely related Government procurement operation, the United States Government thereby incurs no responsibility nor any obligation whatsoever; and the fact that the Government may have formulated, furnished, or in any way supplied the said drawings, specifications, or other data, is not to be regarded by implication or otherwise as in any manner licensing the holder or any other person or corporation, or conveying any rights or permission to manufacture, use, or sell any patented invention that may in any way be related thereto.

Qualified requesters may obtain copies of this report from the Defense Documentation Center (DDC), (formerly ASTIA), Cameron Station, Bldg. 5, 5010 Duke Street, Alexandria 4, Virginia

This report has been released to the Office of Technical Services, U.S. Department of Commerce, Washington 25, D.C., in stock quantities for sale to the general public.

Copies of this report should not be returned to the Aeronautical Systems Division unless return is required by security considerations, contractual obligations, or notice on a specific document.

400 - January 1964 - 162-22-384

FOREWORD

Each year the Aeronautical Systems Division (ASD), Air Force Systems Command (AFSC), sponsors a Science and Engineering Symposium in advance of the Annual Air Force Science and Engineering Symposium. This provides a specific motivation for ASD personnel to prepare papers that reflect the results of their efforts. The variety of subjects also provides an opportunity for interdisciplinary exchange of information that is becoming ever more important.

This year the symposium papers are being published individually to facilitate distribution and retention. However, each paper carries this same foreword which lists the titles of all papers together with the authors and the ASD Technical Documentary Report (TDR) numbers. Readers who are interested in obtaining copies of other papers are urged to contact the authors directly or the Defense Documentation Center, Alexandria, Virginia. It should be noted that certain papers are classified and are available to only those persons having proper security clearances and a "need-to-know."

This paper is one of 21 presented at the "ASD 1963 Science and Engineering Symposium" held at Wright-Patterson Air Force Base, Ohio, 18-19 September 1963. They consist of 17 CONTRIBUTED and 4 INVITED papers, listed below. *The 5 contributed papers that are asterisked were also presented at the 10th Annual Air Force Science and Engineering Symposium held at the Air Force Academy, Colorado Springs, Colorado on 8, 9 and 10 October 1963.

CONTRIBUTED PAPERS

*Operation Fishbowl — Close-In Thermal Measurements, UNCLASSIFIED Title, SECRET-RESTRICTED DATA Paper
F. D. Adams
ASD-TDR-63-691

Radiation Physics: Its Impact on Instrumentation
R. C. Beavin, 1st Lt, USAF
ASD-TDR-63-697

*Application of Aerodynamic Lift in Accomplishing Orbital Plane Change
R. N. Bell, 1st Lt, USAF and W. L. Hankey, Jr., Ph. D.
ASD-TDR-63-693

Controlled Thermonuclear Reactions for Space Propulsion
R. F. Cooper and R. L. Verga
ASD-TDR-63-696

Comparison of Approaches for Sonic Fatigue Prevention
M. J. Cote
ASD-TDR-63-704

Air/Ground Communications Via Orbiting Reflectors
C. C. Gauder
ASD-TDR-63-702

*Ring Laser Techniques for Angular Rotation Sensing
D. A. Guidice and W. L. Harmon
ASD-TDR-63-694

Zero Gravity Pool Boiling
L. M. Hedgepeth and E. A. Zara
ASD-TDR-63-706

An Analytical Study on Liquid Cesium Purification in View of Current and Projected Needs
R. H. Herald
ASD-TDR-63-703

*Preliminary Weight Estimates for Advanced Dynamic Energy Conversion Systems
G. D. Huffman
ASD-TDR-63-705

Force Balance Determination of Inlet Performance for Advanced Vehicle Applications to Orbital Velocities Using Internal Drag Measurements
P. H. Kutschenreuter, Jr.
ASD-TDR-63-701

Thermal Insulations for Aerospace Applications: -423° to + 3000°F
M. L. Minges, 1st Lt, USAF
ASD-TDR-63-699

The Rankine Cycle Air Turboaccelerator (RATA) Engine — A New Cryogenic Engine system, UNCLASSIFIED Title, CONFIDENTIAL Paper
H. E. Pope
ASD-TDR-63-692

How PERT is Used in Managing the X-20 (Dyna-Soar) Program
R. M. Sadow
ASD-TDR-63-698

Liquid Metal Magnetohydrodynamic Power Conversion
G. B. Stafford
ASD-TDR-63-700

System Components Information Center
M. G. Toll
ASD-TDR-63-695

*Aerospaceplane — An Advanced System Planning Study, UNCLASSIFIED Title, SECRET Paper
Alan Watton
ASD-TDR-63-690

The following four invited papers were prepared by the listed authors covering Air Force effort in the subject areas and were presented at the 10th Annual Air Force Science and Engineering Symposium. Copies of these papers may also be obtained from the authors or the Defense Documentation Center.

ASD-TDR-63-693

INVITED PAPERS

Summary of Laminar Flow Control Techniques for Aircraft
P. P. Antonatos, R. X. Mueller and J. P. Nenni
ASD-TDR-63-689

Materials for the Space Age
H. D. Colwick, Capt, USAF, D. H. Cartolano and C. W. Douglass
ASD-TDR-63-688

V/STOL Systems Technology Today and Tomorrow, UNCLASSIFIED Title, SECRET Paper
G. E. Dausman, Joseph Jordan and W. A. Summerfelt
ASD-TDR-63-687

Limited War/COIN, UNCLASSIFIED Title, SECRET Paper
D. A. Rook, Capt, USAF
ASD-TDR-63-686

A large percentage of the above listed authors are with organizational elements that have been or are being transferred from ASD to the recently established Research and Technology Division (RTD). These scientists and engineers from the Air Force Aero-Propulsion Laboratory, Air Force Avionics Laboratory, Air Force Flight Dynamics Laboratory, Air Force Materials Laboratory, and the Systems Engineering Group have, in some cases, prepared the symposium presentations as well as the published documents jointly with technical personnel remaining in ASD.

These 21 papers represent only a small portion of the ASD/RTD effort which spans from basic research through engineering and includes various aspects of technical management. They are illustrative of the competence of our technical personnel and we proudly dedicate them to all our scientists and engineers.

John E. Keto

JOHN E. KETO
Chief Scientist
Aeronautical Systems Division

BIOGRAPHIES

LIEUTENANT ROLAND N. BELL received his B.S. degree in aeronautical engineering in 1959, and his M.S. degree in aerospace engineering in 1961, from the Virginia Polytechnic Institute. In the course of his formal education he was elected to the Sigma Gamma Tau, Tau Beta Pi, Pi Tau Chi, Scabbard and Blade and Arnold Air Society, honorary societies. After entry into the USAF as a Lieutenant, he was assigned to his present position as an aerospace engineer in the Aerodynamics Branch, X-20 (Dyna-Soar) Engineering Office. While in this position he has worked on various segments of the X-20 flight profile including heat transfer during boost and reentry, and the effects of various parameters on lateral and longitudinal range capability. He is the author of an ASD Technical Documentary Report titled A Thermal Analysis of High Speed, High Altitude Ejections published in April 1963 (ASD-TDR-62-592). Lieutenant Bell is also a member of the American Institute of Aeronautics and Astronautics and the Air Force Association.

DR. WILBUR L. HANKEY, JR. received his B.S. degree in aeronautical engineering from Pennsylvania State University in 1951 and possesses M.S. degrees in aeronautical engineering from both the Massachusetts Institute of Technology (1953) and Ohio State University (1958). He obtained the Ph.D. degree in aeronautical and astronautical engineering from the Ohio State University in 1962. Dr. Hankey entered the Air Force as a Lieutenant in 1953 and was assigned to the Transonic Wind Tunnel Unit, Wright Air Development Center, Wright-Patterson Air Force Base (WPAFB), Ohio, where he accomplished a wide range of transonic flow studies. Upon completion of his military tour in 1955, Dr. Hankey continued his work in the Wind Tunnel Branch as an aeronautical research engineer until 1958. At that time he was appointed Chief of the Aerothermodynamics Unit, Hypersonic Flight Section, Aircraft Laboratory, Wright Air Development Division, WPAFB, and remained in that position until December 1959. During this time, Dr. Hankey made detailed studies into hypersonic flow phenomena, especially heat transfer, and published a design handbook, Design Procedures for Computing Aerodynamic Heating at Hypersonic Speeds, WADC-TR-59-610. His doctorate dissertation was on the investigation of hypersonic configurations titled "Optimization of Lifting Reentry Vehicles." In December 1959, Dr. Hankey was appointed Chief of the Aerodynamics Branch, X-20 (Dyna-Soar) Engineering Office. He is presently in charge of systems analysis in the Test and Analysis Division, X-20 Engineering Office. Dr. Hankey belongs to many honorary societies and is a member of the American Institute of Aeronautics and Astronautics.

ABSTRACT

This study considers the concept of a hypersonic glider-type spacecraft utilizing its aerodynamic maneuvering capability in performing orbital plane change. For lifting vehicles an optimization procedure is developed which defines the proper vehicle attitude, propulsion utilization and sequence of operations to produce the maximum plane change for a given fuel expenditure. The results obtained are compared with the fuel requirements for a pure propulsion (nonlifting) plane change while remaining in orbit. Specifically, the optimum bank angle, angle of attack, entry angle, thrust alignment and thrusting procedures are defined. In addition, the advantages of high L/D vehicles are graphically illustrated. The method is seen to be more efficient than the pure propulsion method, but is found to be far more complex and requires longer times to execute.

TABLE OF CONTENTS

ILLUSTRATIONS

ILLUSTRATIONS (CONT'D)

SYMBOLS

a	semi-major axis of an ellipse (ft)
B	$\frac{L_c}{W}\left[1+\left(\frac{L}{D}\right)_{opt}^{-2}\right]$
C_D	drag coefficient
C_L	lift coefficient
ℓ_1	unit angular momentum (ft^2/sec)
ℓ^*	one-half the area swept by a rotating velocity vector in unit time (ft^2)
D	drag (lbs)
e	emissivity (1.0)
g	acceleration of gravity (ft/sec^2) (32.174)
h	altitude above surface of earth (ft)
I_{sp}	specific impulse of rocket motor (sec) (310)
i	orbit inclination measured relative to the equator
L	lift (lbs)
m	vehicle mass (slugs) (initial value 1000)
R_E	earth equatorial radius (ft) (20.9264×10^6)
R_N	nose radius of the vehicle
r	radial distance from center of earth (ft)
S	vehicle reference area (ft^2) (400)
T	temperature ($^\circ F$)
T	thrust (lbs)
t	time (sec)
V	velocity (ft/sec)
W	vehicle weight (lbs)

SYMBOLS (CONT'D)

α	angle of attack (deg)
γ	angle of incidence of velocity vector from a plane tangent to the earth's surface (deg)
Δ	a change in or impulse to a quantity
δ	angle off-center thrust makes with vehicle flight direction in orbital plane (deg)
ϵ	orbit eccentricity
Λ	angle thrust makes with flight path during thrusting turn (deg)
λ	angle of retrograde thrust offset
μ	earth's gravitational constant (ft^3/sec^2) (1.40770×10^{16})
ϕ	vehicle bank angle (deg)
θ	sweep angle of radius vector in orbital plane (deg)
ρ	atmospheric density ($slugs/ft^3$)
ψ	heading angle (deg)

SUBSCRIPTS AND SUPERSCRIPTS

$( )_1$	original orbit value
$( )_2$	value after retrograde impulse
$( )_A$	parametric value at orbit apogee
$( )_c$	circular orbit value
$( )_{deorb}$	deorbit value
$( )_{en}$	value during reentry
$( )_{ex}$	rocket exhaust value (9000 ft/sec)
$( )_{exit}$	atmospheric exit value
$( )_f$	value at completion of action
$( )_i$	value at initiation of action
$( )_{man}$	maneuver value

SYMBOLS (CONT'D)

$( )_{min}$	minimized value of a parameter
$( )_{opt}$	optimum value of a quantity
$( )_{orb}$	quantity needed to reestablish orbit
$( )_{p}$	parameter value at orbit perigee
$( )_{po}$	value at pullout during reentry
$( )_{total}$	total required
$(\dot{})$	time rate of change

I. INTRODUCTION

During space flights of extended duration, or to fulfill specified mission objectives, it will become necessary for future spacecraft to possess an orbital plane change capability. In general, there are two ways in which this may be accomplished: (1) by a pure transverse propulsive thrust while remaining in orbit, or (2) by atmospheric maneuvering utilizing aerodynamic lift and small amounts of selected propulsion after descent from orbit, followed by reascent to orbital altitude. The first method is relatively simple in execution, but expensive in terms of fuel consumption. The second method, titled "synergetic or aeropropulsive maneuvering," can be more economical in its fuel requirements, but is far more complex from a guidance and control standpoint and requires longer durations to execute.

While utilization of the pure propulsion method results in nearly instantaneous plane change, the amount of propellant needed may be restrictively high. For example, assuming a circular orbit of 100 nautical miles altitude, a transverse velocity impulse (which changes the direction but not the magnitude of the original velocity vector) of approximately 447 ft/sec is required for each degree change in the orbital plane angle. While this may not appear excessive at first glance, consider that this means velocity impulses of 4460 ft/sec for a 10-degree plane change and 13,243 ft/sec for a 30-degree plane change. In terms of propellant consumption for a maneuvering system having an I_{sp} = 310 seconds, 0.564 pounds of fuel per pound of inert structure is required for a 10-degree plane change and 2.77 pounds of fuel per pound of inert structure is required for a 30-degree plane change. While plane changes of the magnitudes cited above may not be required in all space missions, the above consideration of the magnitudes of impulse and propellant consumption yields an idea of the problem involved.

The method utilizing atmospheric maneuvering in conjunction with propulsion augmentation, termed the "synergetic" method (Ref. 1), is the subject of this report. Due to the complexity of the maneuver, it must be dealt with in several distinct phases, and is only considered because, properly employed, it is more economical in terms of propellant consumption, a factor of primary importance in present-day technology. This advantage is derived from the fact that for near-earth orbits it is cheaper to alter altitude than direction.

The analysis is performed in separate and distinct steps, and throughout an effort is made to optimize the procedure so that the minimum-energy path is followed as closely as possible. The individual steps comprising the method are (Fig. 1):

(1) retrograde impulse and deorbit;

(2) reentry;

(3) circularization of the orbit while forcing the velocity vector to $\gamma = 0°$;

(4) thrusting, banked turn within the atmosphere during which the major portion of the plane change is accomplished;

(5) velocity impulse sufficient to exit the atmosphere and return to the original orbital altitude; and

(6) velocity impulse to circularize and reestablish the orbit.

It is the purpose of this report to ascertain whether the added complexity and time requirement of this method can be justified in terms of the quantity of propellant saved.

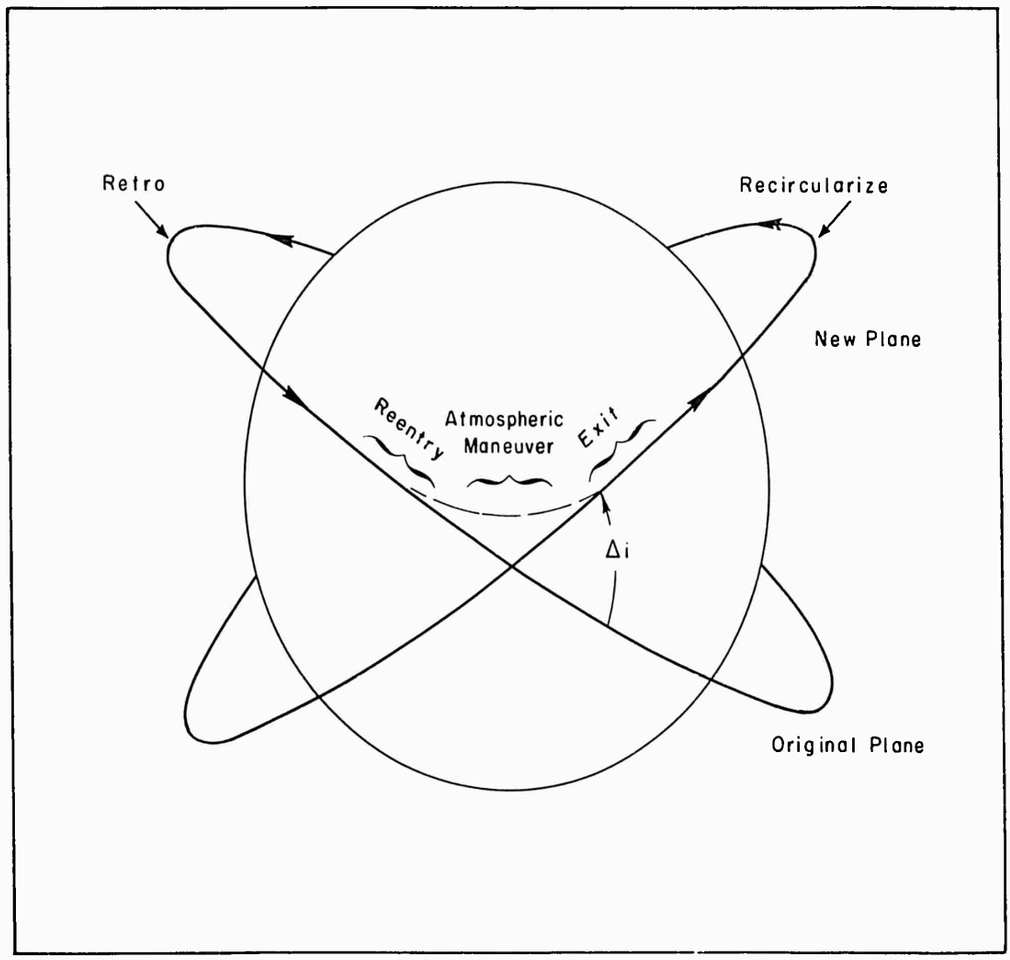

Figure 1. Schematic of Synergetic Maneuver

II. ANALYSIS

Before starting the actual analysis, it is necessary to list certain assumptions which govern the entire investigation. It is assumed first, that an accurately throttleable, multi-start-capability rocket engine is available; second, that thrust applications in space, to circularize the orbit after reentry and to exit the atmosphere, result in instantaneous velocity and/or direction changes; third, that the vehicle is stable (ac = cg) so that no allowance is necessary for thrust vector control; and fourth, the chosen L/D ratios are attainable by present or proposed spacecraft. Since each step in the maneuver is a separate entity, each is treated as such and the resultant velocity increments summed to yield the total propulsion requirements for a given plane change magnitude. In an effort to present as thorough a study as possible, covering the greatest variety of circumstances, the following conditions are assumed throughout the report:

(1) the original orbital altitude is 100 nautical miles since Reference 1 shows that lower orbital altitudes are more efficient for synergetic maneuvering and this is a reasonable minimum from an orbital lifetime standpoint;

(2) the aerodynamic characteristics may be expressed by Newtonian techniques (Appendix I);

(3) the original vehicle weight and reference area remain the same for all L/D values since variations in these parameters result in small performance changes as shown in Appendix II;

(4) no thermal or structural limitations exist. (However, maximum temperatures during the maneuver are presented for comparative purposes.)

DEORBIT PHASE

From a 100-nautical mile circular orbit, a deorbit is required such that the vehicle reaches 300,000 feet at a specified reentry angle with minimum energy loss. The minimum-energy-loss transfer between coplanar orbits has been shown (Ref. 2) to be a Hohmann transfer ellipse with apogee and perigee tangent to the original and final orbits respectively. The retrograde velocity necessary, and the resultant entry velocity for this maneuver can be calculated from the Keplerian equations (Ref. 3) with negligible error. From the constancy of energy and angular momentum at any point on a given orbit, one obtains

$$\frac{V_2^2}{2} - \frac{\mu}{r_2} = \frac{V_{en}^2}{2} - \frac{\mu}{r_{en}} \tag{1}$$

and

$$r_2 V_2 = r_{en} V_{en} \cos \gamma_{en} . \tag{2}$$

Combining these equations, recognizing that $r_2 = r_1$, and solving for the entry velocity, V_{en}, obtain

$$V_{en} = V_{c_1} \sqrt{\frac{2\left(\frac{r_1}{r_{en}} - 1\right)}{1 - \left(\frac{r_{en}}{r_1} \cos \gamma_{en}\right)^2}} \tag{3}$$

where

$$V_{c_1} = \sqrt{\frac{\mu}{r_1}} \quad .$$

Using Equation (3), the entry velocity at 300,000 feet, after descent from a 100-nautical mile circular orbit, may be calculated for the specified entry conditions. Then, from Equation (2) the value of V_2 is obtained. Thus, the retrograde impulse required is, by definition

$$\Delta V = V_1 - V_2 \quad . \tag{4}$$

To ascertain that this is the minimum ΔV value, consider the following sketch:

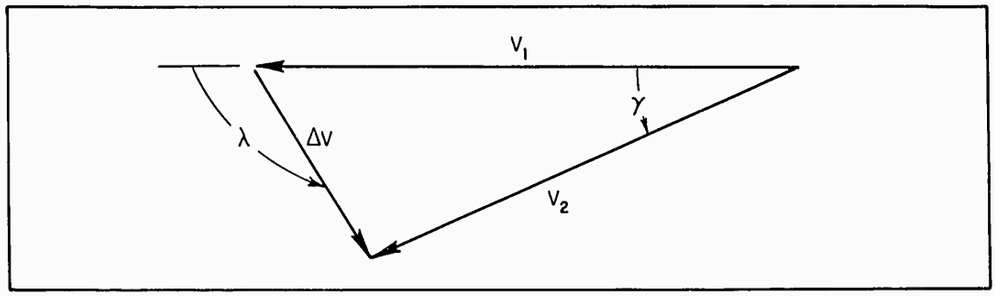

From this sketch

$$V_2 \cos\gamma = V_1 + \Delta V \cos\lambda \, . \tag{5}$$

For any orbit, the constancy of angular momentum yields

$$r \, V \cos\gamma = \text{Constant} \, . \tag{6}$$

Therefore

$$r_2 \, V_2 \cos\gamma = r_{en} \, V_{en} \cos\gamma_{en} \tag{7}$$

Combining Equations (5) and (7) obtain

$$\Delta V = \frac{\left(\frac{r_{en}}{r_1} V_{en} \cos\gamma_{en}\right) - V_1}{\cos\lambda} \quad . \tag{8}$$

Since the conditions at the time of retrofire are fixed by the original orbit and those at atmospheric entry are established by definition, Equation (8) may be rewritten as

$$\Delta V = \frac{\text{Constant}}{\cos\lambda} \quad . \tag{9}$$

Thus, if $|\Delta V|$ is to be a minimum for a given reentry, then $|\cos\lambda|$ must be a maximum, or

$$\lambda = 180^\circ , \tag{10}$$

a pure retrograde impulse.

The value of the retrograde impulse obtained by Equations (3) and (4) is shown in Figure 2. These values, then, are the minimum velocity impulses necessary to perform the deorbit maneuver.

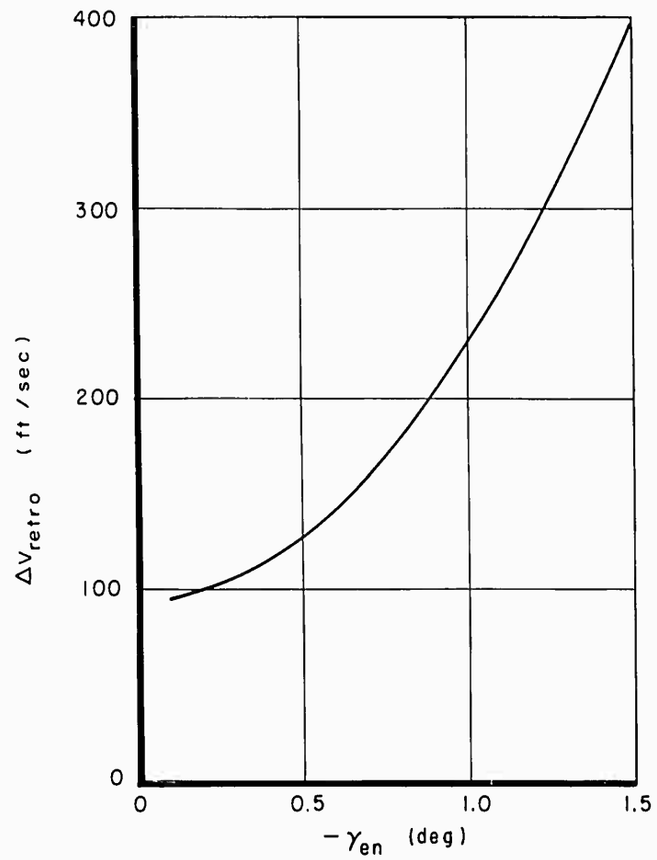

Figure 2. Variation of Retrovelocity with Entry Angle (100-NM Orbit)

REENTRY PHASE

At an altitude of 300,000 feet aerodynamic effects become appreciable and it is necessary to use more refined techniques in the analysis. It is also desirable to know what reentry procedures will lead to minimum energy dissipation for a given plane change; that is, what bank angle, entry angle, angle of attack and pullout procedure will require the least amount of propulsion to attain the same results. To take all of the possibilities into account, computer programs were set up based on the entry angles and velocities obtained from the DEORBIT PHASE analysis. Cases were run for several reentry angles from -0.1° to -1.5°, at various bank angles from 0° to 90° and for various angles of attack based on

$(L/D)_{max}$ values from 1 to 4. The aerodynamic characteristics for the chosen $(L/D)_{max}$ values were computed by means of Newtonian aerodynamics as presented in Appendix I. The results of the computer runs defined the optimum angle of attack and bank angle for the reentry phase as shown in Figures 3 and 4 respectively. A comparison of Figures 3 and I-1 shows that the optimum angle of attack for the reentry phase is that for $(L/D)_{max}$.

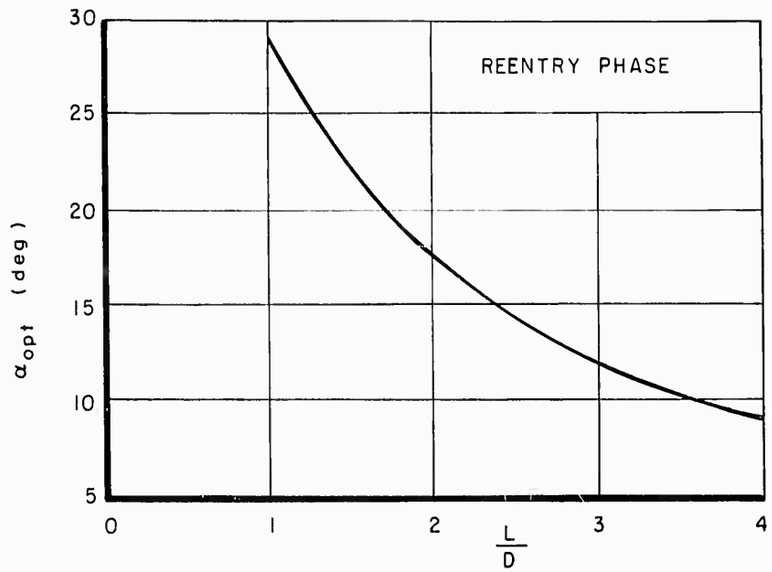

Figure 3. Optimum Angle of Attack Versus L/D

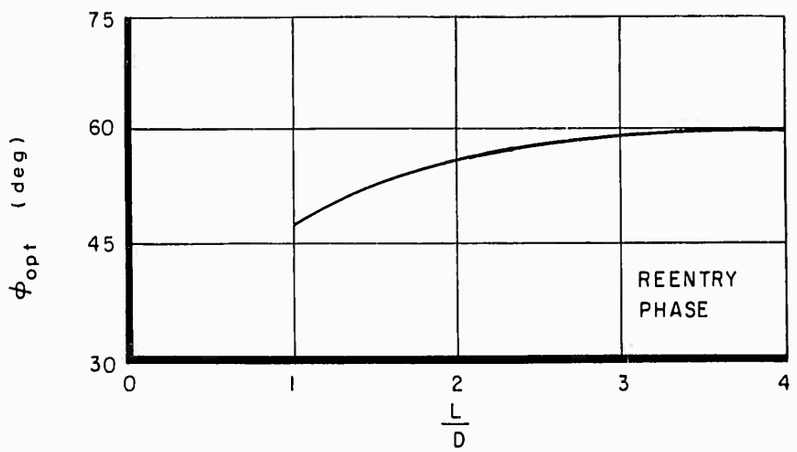

Figure 4. Optimum Bank Angle Versus L/D

The above reentry conditions were run to pullout, or $\gamma = 0°$. After considering this data it was felt a more economical pullout maneuver could be effected in light of the magnitude of the velocity impulse required before the next phase of the maneuver could be accomplished. At selected points during reentry, the velocity impulse was computed which placed the vehicle at circular speed and $\gamma = 0°$ by using the law of cosines,

$$\Delta V = \sqrt{V^2 + V_c^2 - 2V\ V_c\ \cos\gamma} \tag{11}$$

where

V = local inertial velocity

V_c = local circular velocity

γ = local flight path angle.

These velocity impulses were calculated, and the minimum determined, thus defining the pullout altitude and the starting point for the next phase of the analysis. Figure 5 presents the pullout flight path angle and Figure 6 is a plot of pullout altitude versus entry angle for the various L/D values for ϕ_{opt} and α_{opt}. These values were defined by the point of minimum velocity impulse for circularization which is shown in Figure 7. A point of note in Figure 7 is the plotting of negative velocity impulses. These are recognized as improper, and are merely a result of interpretation. The cases in which they occur reached $\gamma = 0°$ aerodynamically and hence the impulse served only to slow the vehicle to circular speed. In practice this is not done, but the turn is performed at supercircular speed and the excess serves to reduce the impulse needed to exit the atmosphere. The heading change accomplished during reentry is shown in Figure 8. After pullout is completed, the major portion of the plane change must be undertaken.

ATMOSPHERIC MANEUVERING PHASE

After pullout, the atmospheric maneuvering begins in order to accomplish the major portion of the plane change. As suggested in Reference 1, thrust is maintained equal to drag during the atmospheric maneuvering so that no velocity loss is incurred. This procedure results in a thrusting banked turn at constant velocity, angle of attack, flight path angle and bank angle.

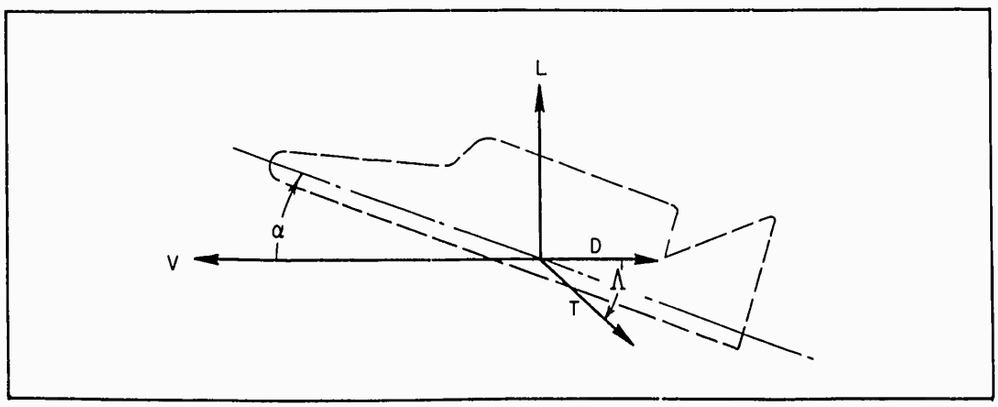

Considering the above sketch, the basic equations governing the aerodynamic maneuver are

$$mV\dot{\psi}\cos\gamma = L\sin\phi + T\sin\Lambda\sin\phi \tag{12}$$

$$mV\dot{\gamma} = \frac{mV^2\cos\gamma}{R_E} + L\cos\phi - mg\cos\gamma + T\sin\Lambda\cos\phi \tag{13}$$

$$m\dot{V} = -D - mg\sin\gamma + T\cos\Lambda \tag{14}$$

$$T = -\dot{m}V_{ex} = \dot{m}V_{effective} \tag{15}$$

or

$$dV_{effective} = V_{ex}\,d(\ell n\, m)\,. \tag{16}$$

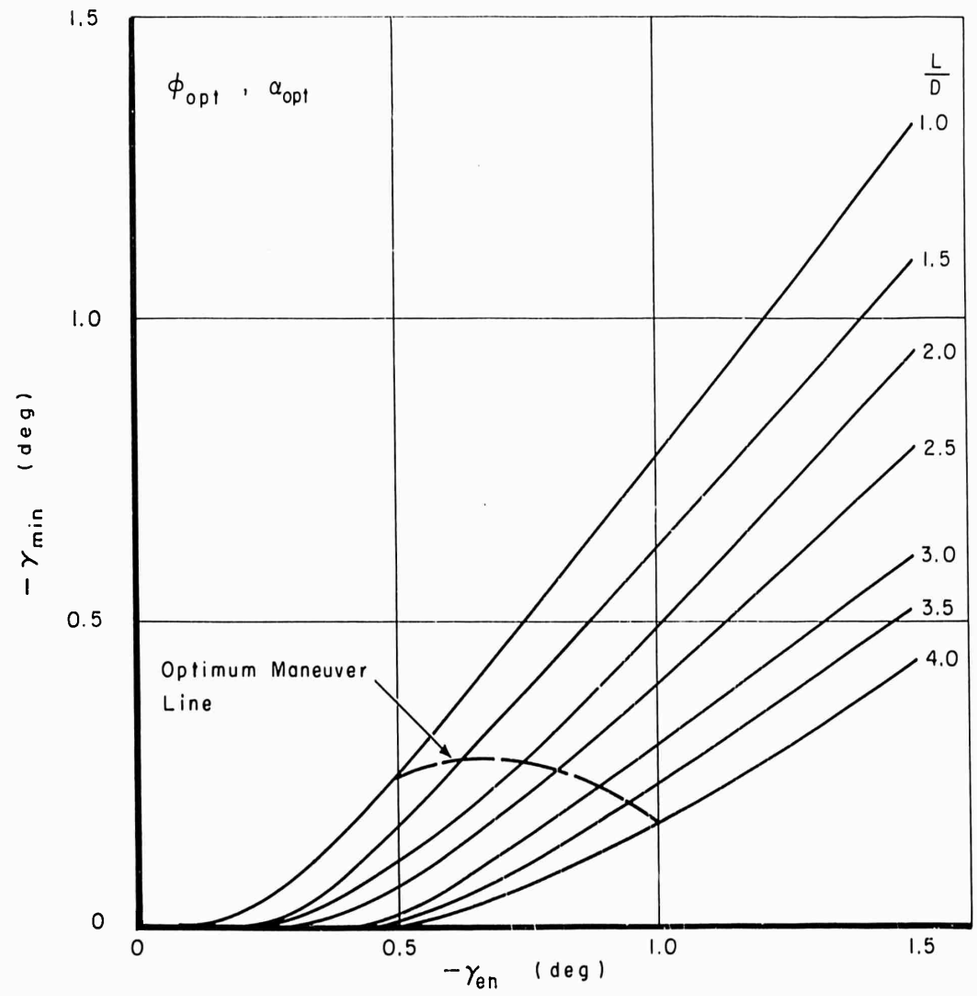

Figure 5. γ for Minimum ΔV Versus Entry γ for Various L/D Values

For the case under consideration, the following conditions hold:

$$\gamma = 0, \qquad \dot{\gamma} = 0, \qquad \dot{V} = 0 \ .$$

Using these conditions, Equations (12), (13), and (14) may be simplified to

$$\dot{\psi} = \frac{L}{mV} \sin\phi + \frac{T}{mV} \sin\Lambda \sin\phi \tag{17}$$

$$(L + T \sin\Lambda) \cos\phi = m \frac{V_c^2}{R_E} \left(1 - \frac{V^2}{V_c^2} \right) \tag{18}$$

$$D = T \cos\Lambda \ . \tag{19}$$

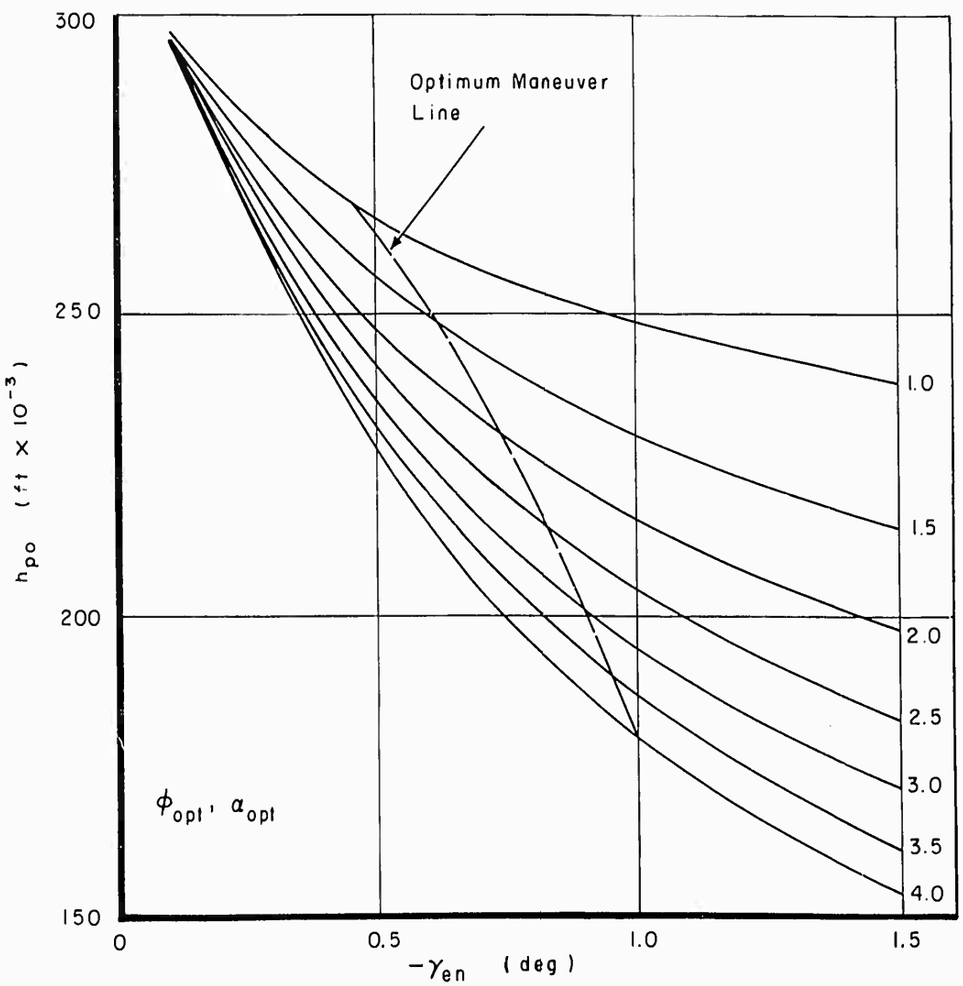

Figure 6. Altitude for Minimum ΔV Versus Entry γ for Various L/D Values

Employing the identity

$$\dot{\psi} = \frac{d\psi}{dt} = \frac{d\psi}{dm}\,\frac{dm}{dt} \tag{20}$$

and using Equation (15), Equation (17) can be written, after some manipulation as

$$\frac{d\psi}{-d(\ell n\ m)} = V_{ex}\left[\frac{L}{D}\cos\Lambda + \sin\Lambda\right]\frac{\sin\phi}{V} \quad . \tag{21}$$

The greatest change in ψ for minimum fuel expenditure may be obtained by differentiating Equation (21) with respect to the independent variables. Differentiation with respect to Λ produces the following optimum:

$$\cot\Lambda_{opt} = \frac{L}{D} \quad . \tag{22}$$

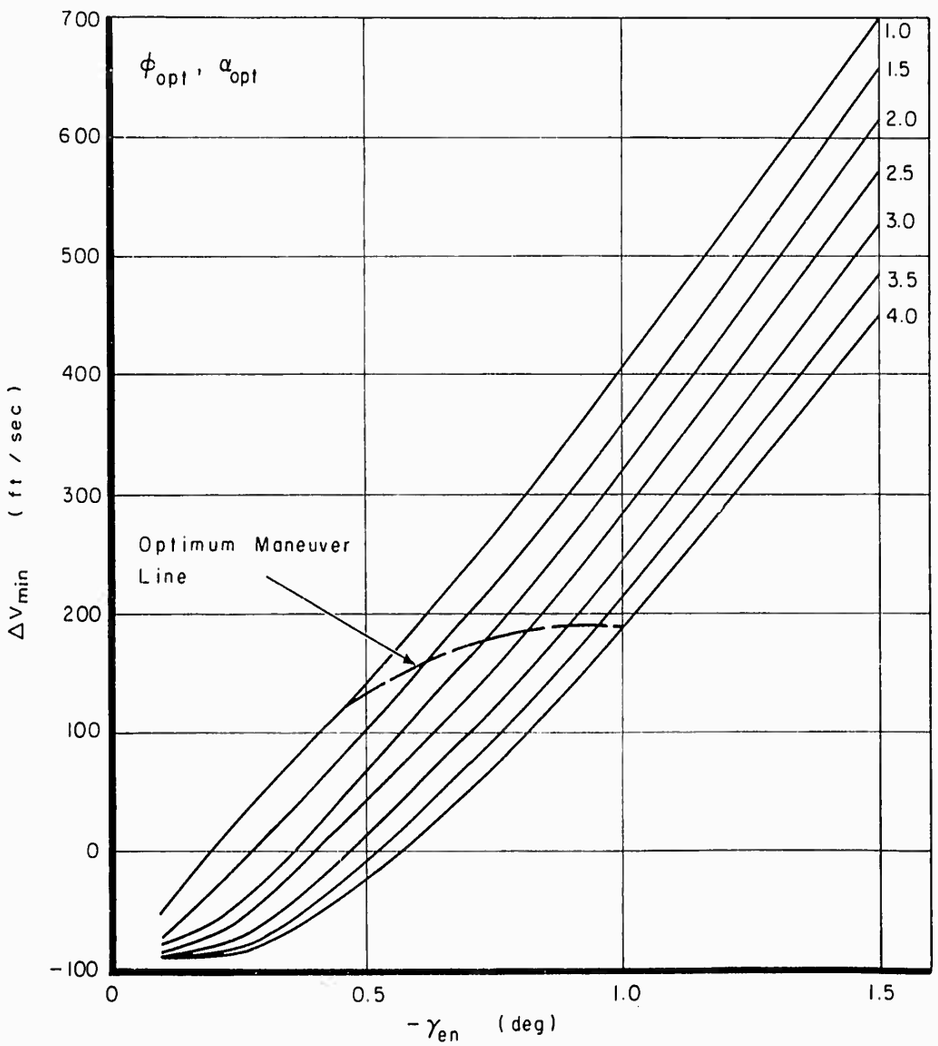

Figure 7. Minimum ΔV Required to Circularize Orbit During Reentry for Various L/D Values

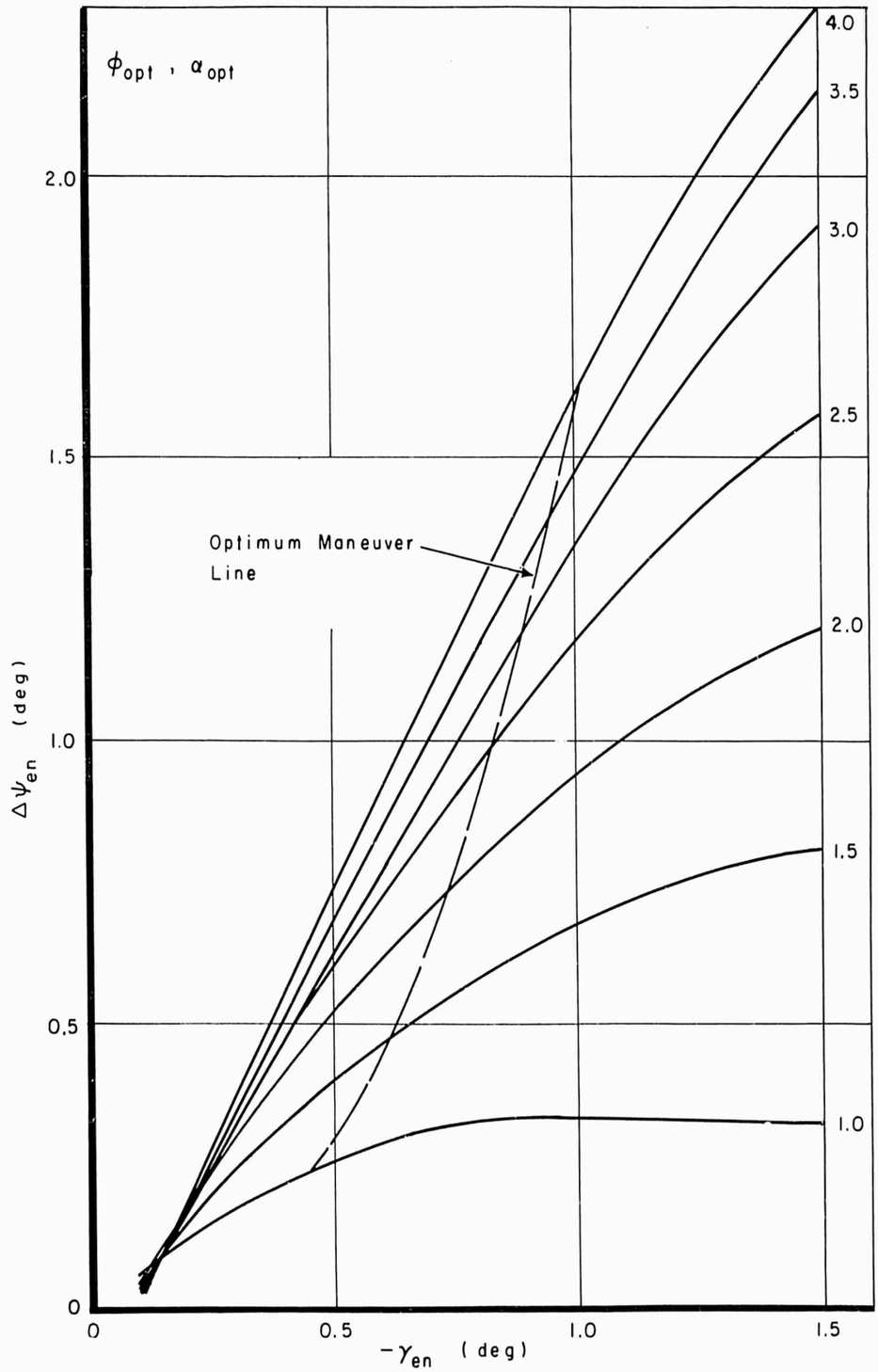

Figure 8. Change in Heading During Reentry for Various L/D Values

Using Equation (22), Equation (21) becomes

$$\frac{d\psi}{-d(\ell n\ m)} = V_{ex}\sqrt{\left(\frac{L}{D}\right)^2 + 1}\ \ \frac{\sin\phi}{V}\ . \tag{23}$$

It is now apparent that the most efficient turning rate may be achieved by flying at $(L/D)_{max}$ or α_{opt}. The optimum values of α and Λ are listed in Table 1 and in Figures I-1 and 9 respectively, for various L/D values.

TABLE 1

OPTIMUM Λ VALUES

$\frac{L}{D}$	α_{opt} (degrees)	Λ_{opt} (degrees)	$\Lambda_{opt} - \alpha_{opt}$ (degrees)
1	29.25	45.00	15.75
1.5	22.17	33.67	11.50
2	17.51	26.57	9.06
2.5	14.35	21.8	7.45
3	12.20	18.47	6.27
3.5	10.6	15.95	5.35
4	9.35	14.03	4.68

Thus for maximum performance, the engine should be placed in the vehicle declined from the vehicle centerline at an angle of $(\Lambda_{opt} - \alpha_{opt})$.

Referring to Equation (23), it is noted that $\sin\phi/V$ must also be maximized for peak efficiency. Equations (18) and (19) may be used to eliminate V from Equation (23). Thus

$$\frac{d\psi}{-d(\ell n\ m)} = V_{ex}\sqrt{\left(\frac{L}{D}\right)^2_{opt} + 1}\ \ \frac{\sin\phi}{V_c}\ (1 + B\cos\phi)^{1/2} \tag{24}$$

where

$$B = \frac{L_c}{W}\left[1 + \left(\frac{L}{D}\right)^{-2}_{opt}\right]$$

and

$$L_c = \frac{1}{2}\rho V_c S C_{L_{opt}}\ .$$

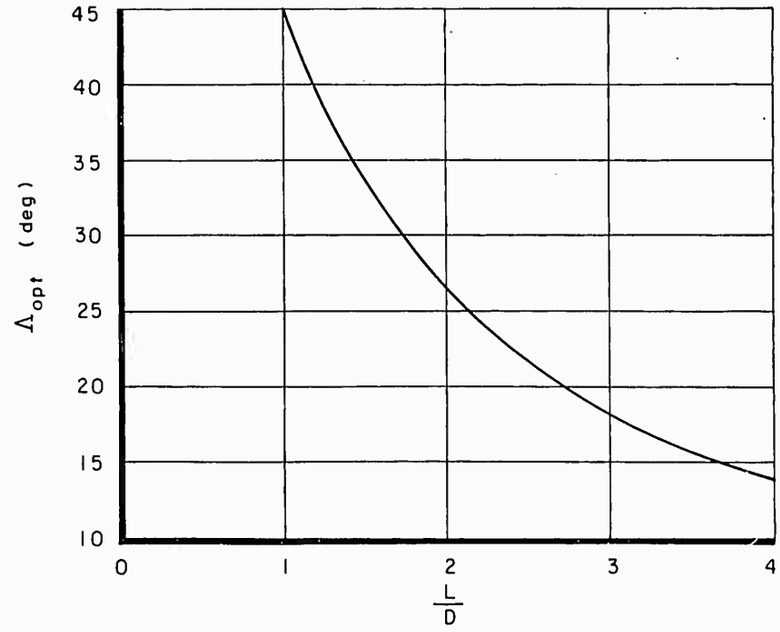

Figure 9. Optimum Thrusting Angle Versus L/D

Differentiation of Equation (24) with respect to ϕ produces

$$\cos\phi_{opt} = -\frac{1}{3B} + \sqrt{\left(\frac{1}{3B}\right)^2 + \frac{1}{3}} \quad . \tag{25}$$

From Equation (25) the variation in ϕ_{opt} with B was calculated and the results presented in Figure 10. The dependency of ϕ_{opt} on altitude and L/D was also computed and plotted in Figure 11. Thus, substitution of ϕ_{opt} from Figure 11 into Equation (24) results in the maximum turn for a given fuel expenditure. Utilizing Equation (16), Equation (24) becomes

$$\frac{\Delta\psi}{\Delta V_{eff}} = \sqrt{\left(\frac{L}{D}\right)^2_{opt} + 1} \quad \frac{\sin\phi_{opt}}{V_c} \quad \left[1 + B\cos\phi_{opt}\right]^{1/2} \tag{26}$$

which is plotted in Figure 12.

EXIT PHASE

After a prescribed heading change has been achieved, a velocity impulse must be added sufficient in magnitude to propel the vehicle from the atmosphere on an elliptical path having an apogee at 100 nautical miles. To maintain the concept of minimum energy expended, the vehicle must exit the atmosphere on a Hohmann transfer ellipse. The optimum bank angle and angle of attack for reentry were also adopted for the ascent phase. The velocity impulse required to insert the vehicle on the proper Hohmann transfer ellipse after completion of atmospheric maneuvering could not be determined by a direct method.

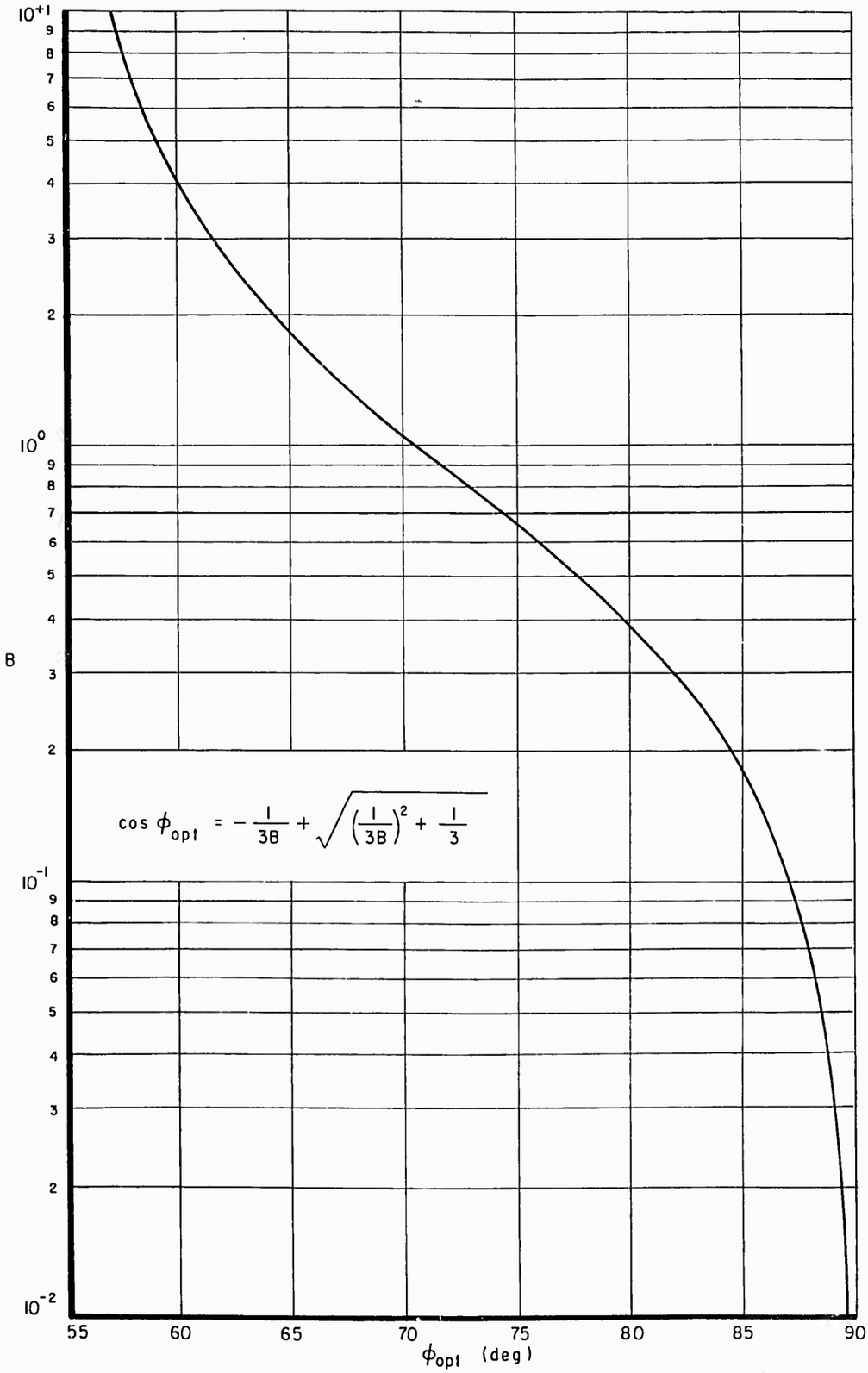

Figure 10. Optimum Bank Angle Defined by Flight Conditions for Atmospheric Maneuvering Phase

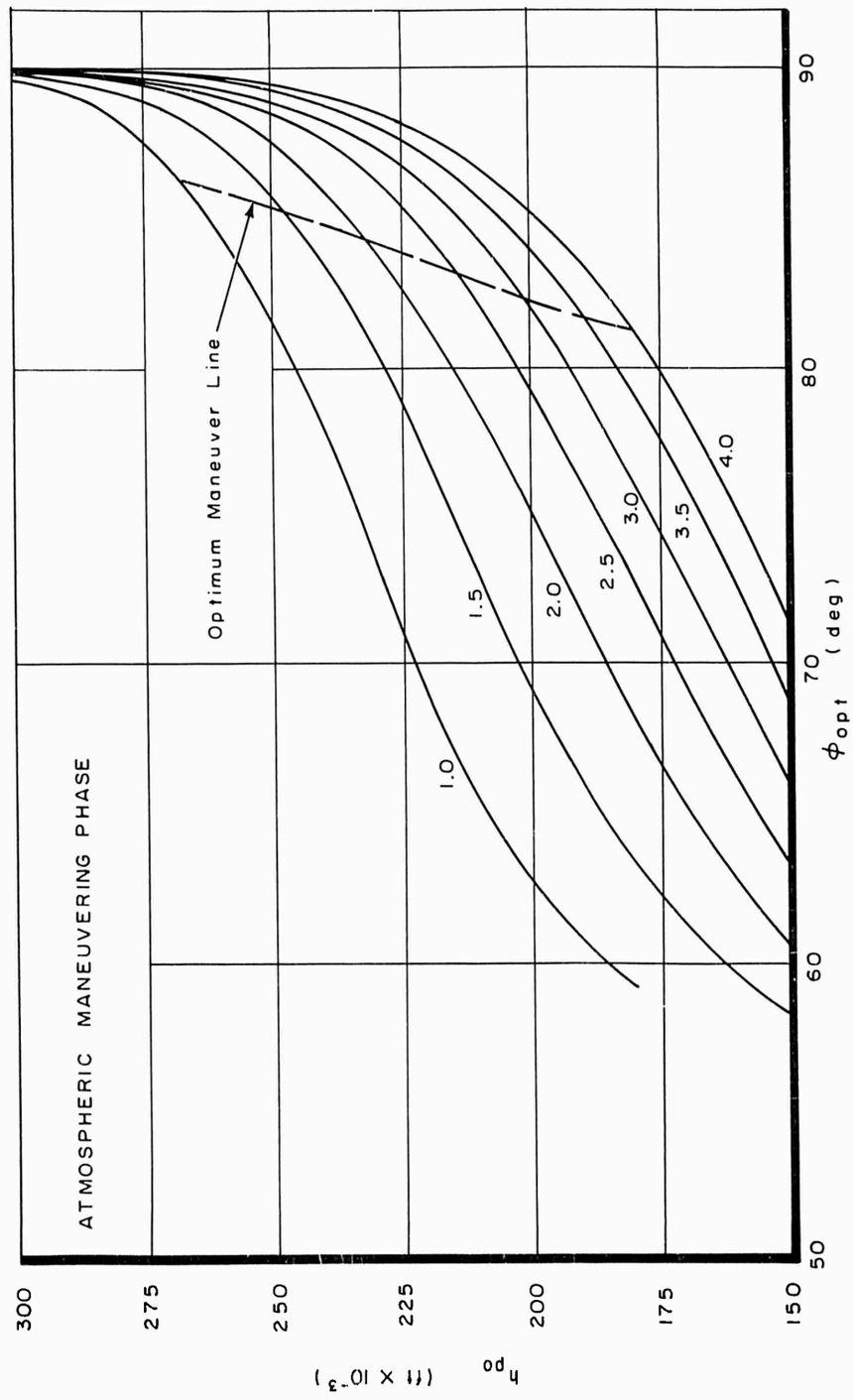

Figure 11. Optimum Bank Angle Versus Pullout Altitude for Various L/D Values

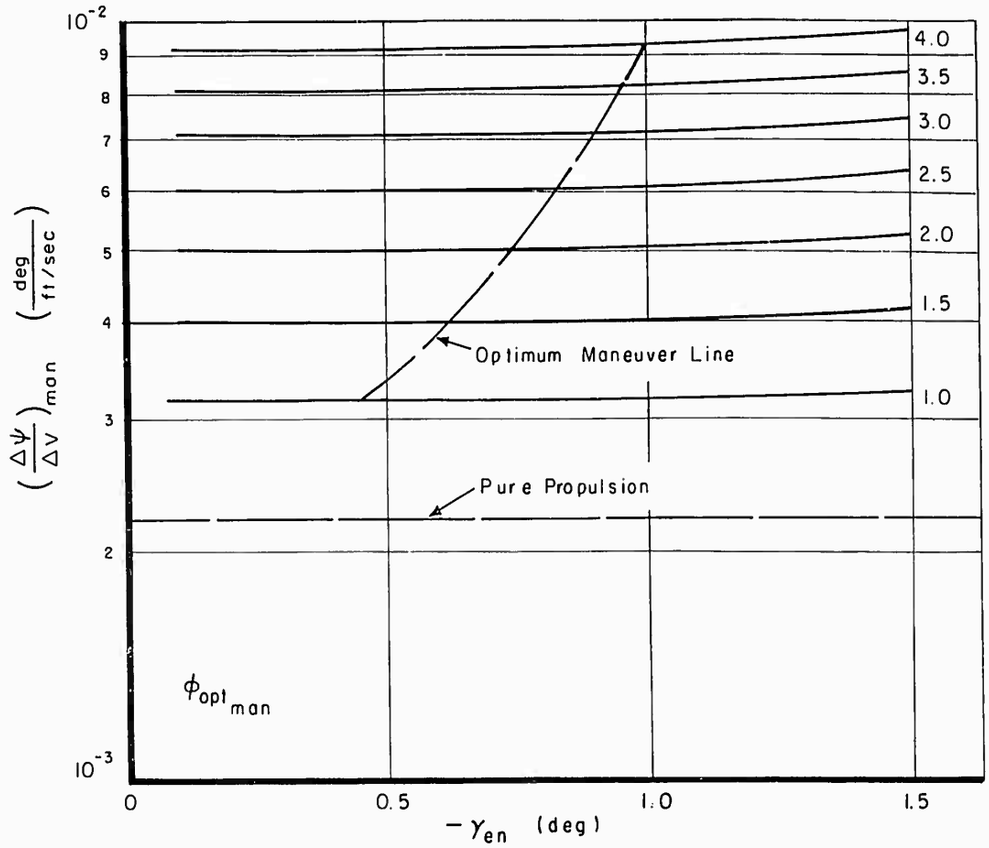

Figure 12. Plane Change Efficiency During Thrusting Banked Turn for Various L/D Values

Therefore, a solution was obtained by an iteration technique in which the exit trajectory and Hohmann transfer ellipse equations were solved simultaneously. The results of this analysis in terms of velocity requirements are plotted in Figure 13. The heading change for the exit phase is shown in Figure 14.

ORBIT REESTABLISHMENT PHASE

Once the proper exit conditions are obtained it is a simple task to calculate the apogee velocity of the resultant ellipse using Equation (2) subscripted for exit conditions. The difference between this calculated value and the known circular velocity, then, is the required recircularization velocity impulse which completes the maneuver. This velocity increment is given in Figure 15.

COMBINATION OF PURE PROPULSION AND AERODYNAMIC TURN

Throughout the preceding analyses, the most efficient turning path was sought and followed. Consider now the application of additional thrust normal to the orbital plane, thus obtaining small increments of $\Delta\psi$ while deorbiting, circularizing, ascending and reestablishing orbit. The advantage is readily apparent if one considers a 30° right triangle in

which a transverse ΔV of 0.500 is obtained for a modest reduction of the longitudinal ΔV to 0.866 for the same total velocity increment.

Keeping the above in mind, an optimization of this principle is attempted. Consider the following sketch.

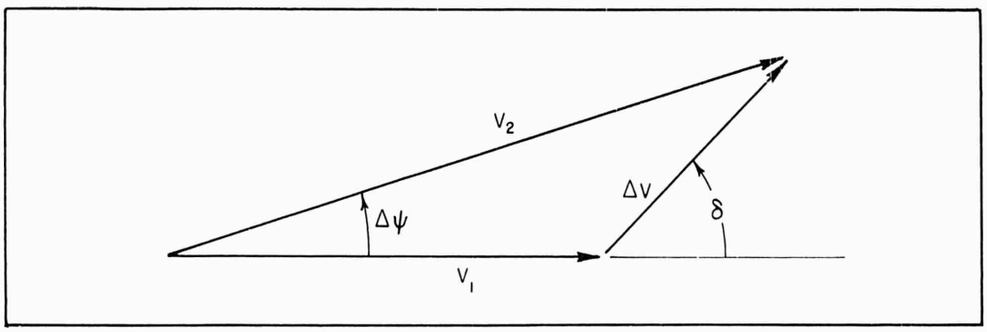

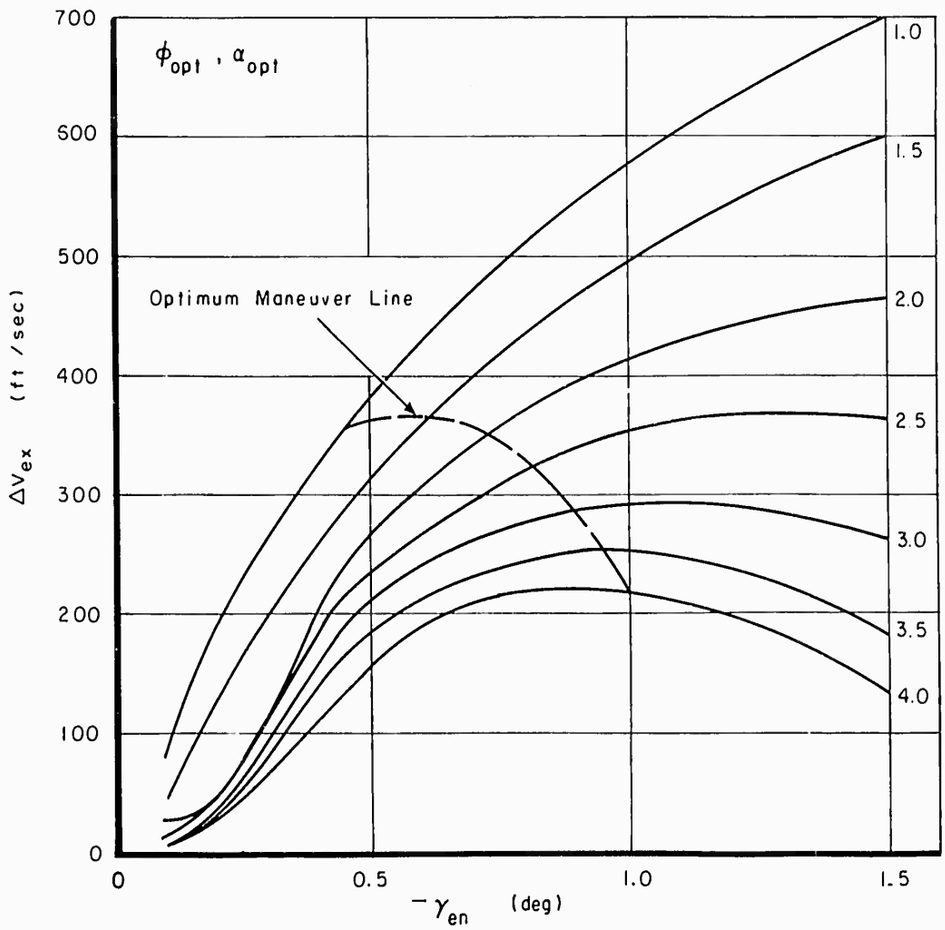

Figure 13. Velocity Impulse Required to Exit Atmosphere and Reach 100-NM Apogee for Various L/D Values

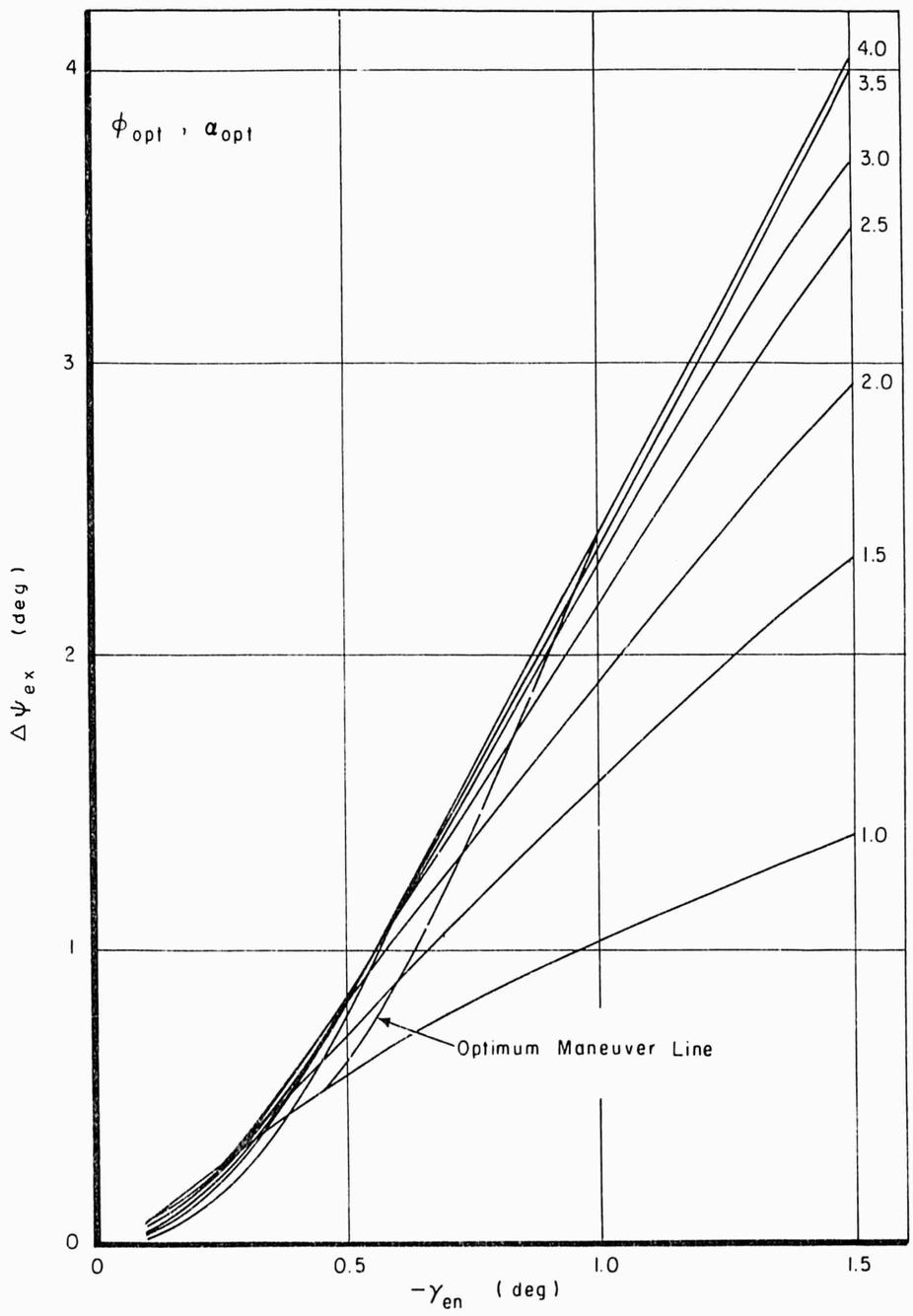

Figure 14. Heading Change During Exit for Various L/D Values

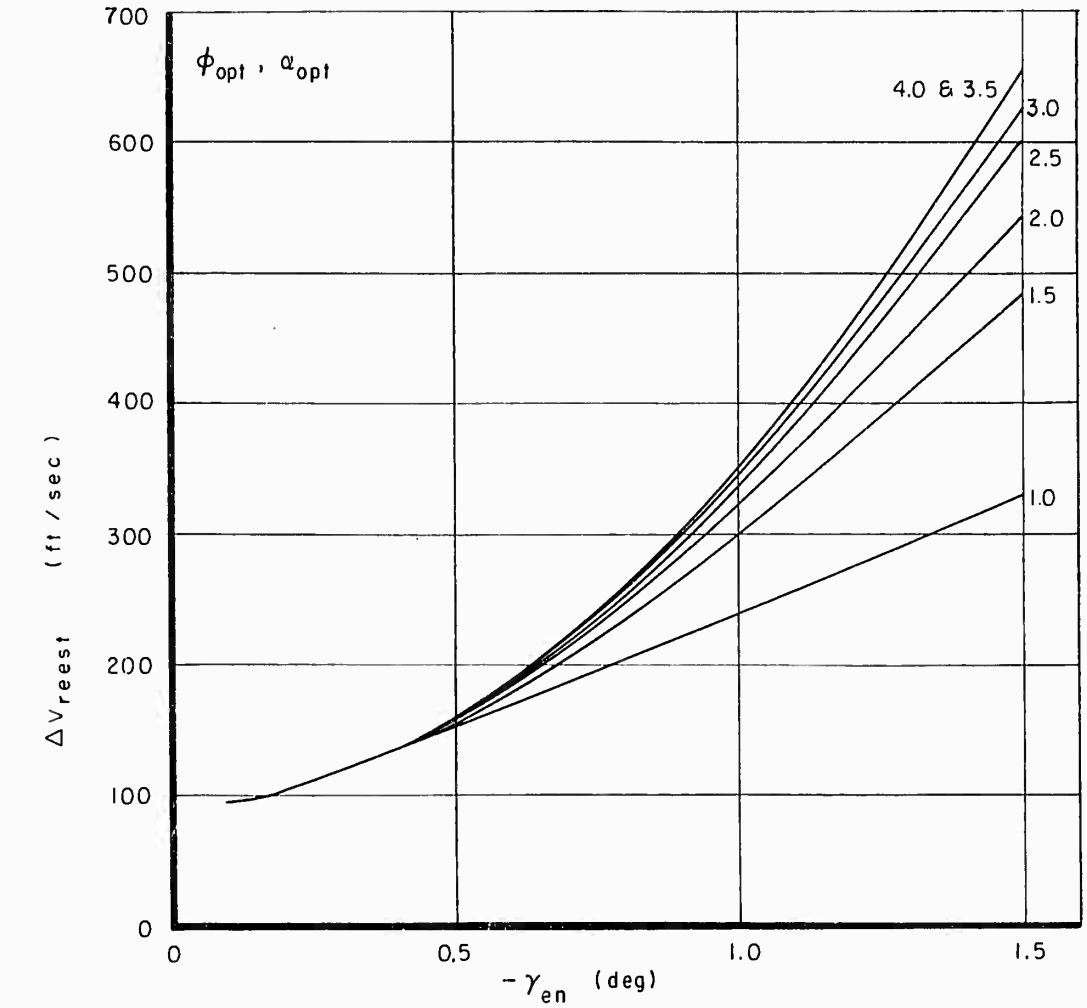

Figure 15. Velocity Impulse Required to Reestablish the Orbit (100 NM) for Various L/D Values

From V_1, a new velocity V_2 is to be obtained such that $\Delta\psi/\Delta V$ is a maximum. Thus, from the preceding sketch

$$V_2 \sin\Delta\psi = \Delta V \sin\delta \tag{27}$$

and

$$V_1 + \Delta V \cos\delta = V_2 \cos\Delta\psi \ . \tag{28}$$

For an optimum maneuver,

$$\left(\frac{\Delta\psi}{\Delta V}\right)_{total} = \text{maximum}. \tag{29}$$

Thus, $(\Delta\psi/\Delta V)_{total}$ is composed of the impulse terms and the aerodynamic turning term or

$$\left(\frac{\Delta\psi}{\Delta V}\right)_{total} = \frac{\left(\frac{\Delta\psi}{\Delta V}\right)_{imp} \Delta V_{imp} + \left(\frac{\Delta\psi}{\Delta V}\right)_{aero} \Delta V_{aero}}{\Delta V_{imp} + \Delta V_{aero}} \quad . \tag{30}$$

Then, from Equations (27) and (26)

$$\Delta\psi \approx \frac{\sin\delta}{V_2} \Delta V_{imp} + \frac{\sqrt{1+\left(\frac{L}{D}\right)^2}}{V_c} \Delta V_{aero} \tag{31}$$

where, in Equation (26) the value of ϕ_{opt} is taken as 90° and in Equation (27) small angles of $\Delta\psi$ are assumed. Also, from Equation (28)

$$\Delta V_{imp} \approx \frac{V_2 - V_1}{\cos\delta} \tag{32}$$

and by definition

$$\Delta V_{aero} = \Delta V_{total} - \frac{V_2 - V_1}{\cos\delta} \quad . \tag{33}$$

Using Equations (31) and (32), Equation (30) may be written as

$$\Delta\psi = \tan\delta \frac{V_2 - V_1}{V_2} + \frac{\sqrt{1+\left(\frac{L}{D}\right)^2}}{V_c} \Delta V_{total} \left[1 - \frac{V_2 - V_1}{\Delta V_{total} \cos\delta}\right] . \tag{34}$$

Maximizing $\Delta\psi$ for a specific ΔV_{total} with respect to δ yields,

$$\sin\delta_{opt} = \frac{V_c}{V_2 \sqrt{1+\left(\frac{L}{D}\right)^2}} \tag{35}$$

or

$$\cot\delta_{opt} \approx \left(\frac{L}{D}\right)_{opt} \tag{36}$$

where $V_2 \approx V_c$ has been assumed.

Thus, using Equation (35), the optimum angle to offset the thrust is defined and these values are shown in Figure 16. It was found, because of the complex orbital parameter interactions, that this offset may be efficiently used only during pullout and exit and not during deorbit and reestablishment as was first assumed. The velocity requirement and the heading change obtained by thrust offset at pullout and exit are shown in Figures 17 and 18 respectively.

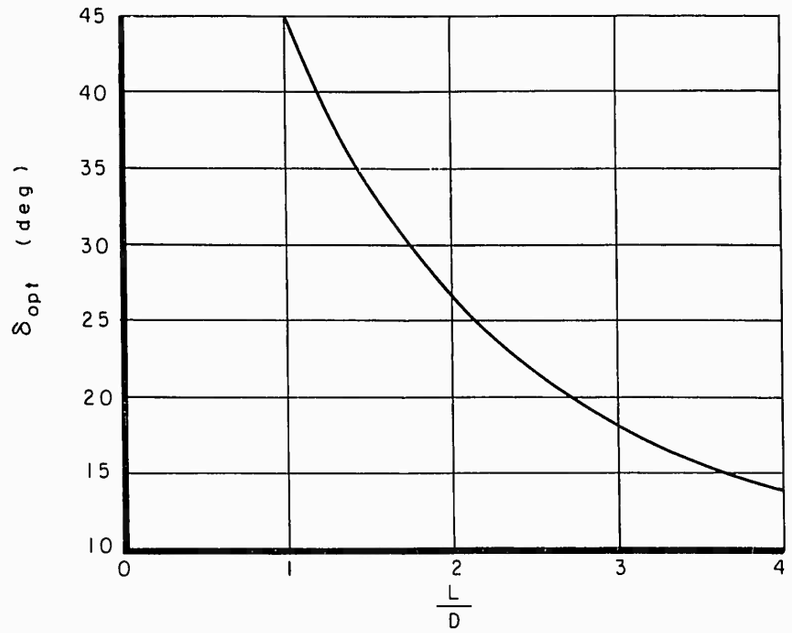

Figure 16. Optimum Angle to Offset Thrust Versus L/D

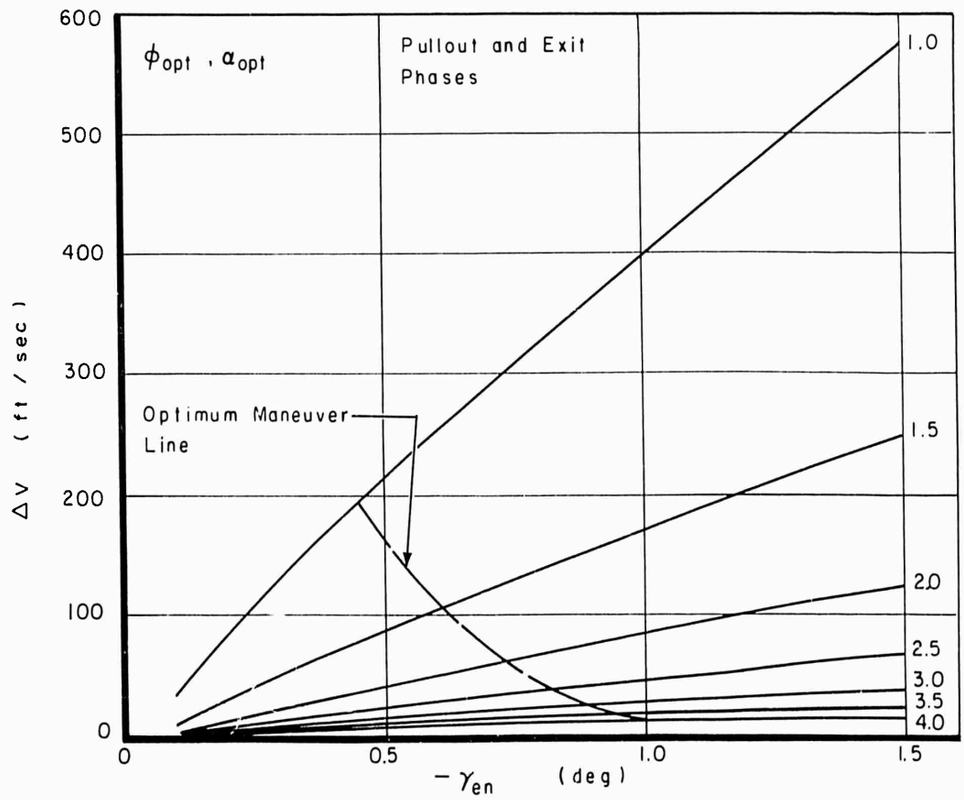

Figure 17. Additional Velocity Required by Thrust Offset for Various L/D Values

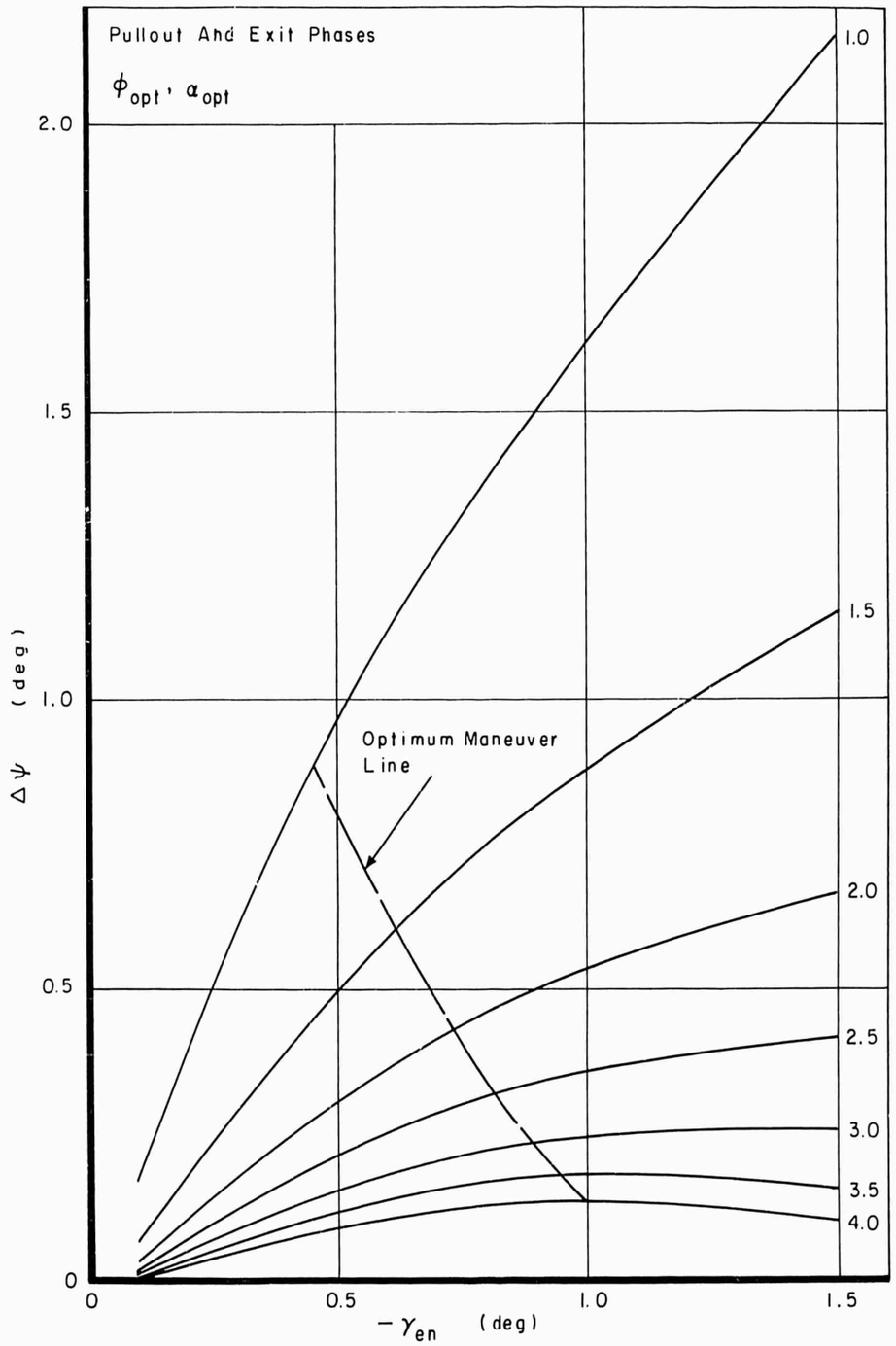

Figure 18. Heading Change Due to Thrust Offset for Various L/D Values

III. DISCUSSION OF RESULTS

At this point the conclusions reached in the Analysis Section on the most efficient technique for accomplishing the orbital plane change are summarized. As pointed out in that section, a pure retrovelocity impulse yields the most economical reentry in terms of propellant consumption. This lends further support to the conclusion that it is easier to alter altitude than direction while in near-earth orbits. As reentry begins, however, it is necessary to consider the effects of entry angle and vehicle attitude on the various flight parameters. This was done through the use of a computer programmed parametric study.

The variation in retrovelocity required to enter at a given flight path angle is shown in Figure 2. It is seen to increase sharply for entry angles steeper than -0.5°. Figure 3 shows the optimum angle of attack, and Figure 4 shows the optimum bank angle which define the optimum entry attitudes. Under these conditions, a variety of $(L/D)_{max}$ and entry angles were run on the computer and the resulting performance is shown in Figures 5 through 8. Notice in Figure 5 that it is advantageous to force the velocity vector to $\gamma = 0°$ before it occurs naturally, though for increasing L/D one may wait longer and take advantage of the heading change being achieved without using thrust. Note, also, that the higher L/D value causes the vehicle to penetrate more deeply into the atmosphere (Fig. 6), yet it retains more energy (Fig. 7) permitting a higher plane change efficiency.

In considering the aerodynamic maneuvering portion of the flight, two facts become readily apparent. First (Fig. 10), steeper optimum bank angles result from low lift-to-weight ratios and high L/D values. Second (Fig. 12), this combination results in greater plane change efficiency by reducing drag losses and directing more of the lift force toward plane change and less toward keeping the vehicle airborne. Also apparent from Figure 12 is the fact that atmospheric plane change efficiency varies nearly linearly with increasing L/D.

Since the higher L/D vehicles penetrate more deeply into the atmosphere, it might be assumed that a greater velocity impulse would be required to exit the atmosphere. Such is not the case, as seen in Figure 13. Despite the deeper penetration, substantially less impulse is required to free it from the atmosphere due to the low drag coefficient of the high L/D vehicles. Part of the advantage accumulated by the higher L/D vehicles is erased by the velocity requirement for orbital reestablishment, however, as seen in Figure 15. While a substantial increase does exist, it is by no means excessive and does not greatly affect the overall efficiency which appears to be inherent in high L/D vehicles.

The advantage gained by offsetting the thrust is seen to be greatest for lower L/D values, diminishing noticeably as L/D increases (Fig. 16). This advantage is taken into account in the succeeding steps which define the optimum flight path for each L/D value.

The total velocity impulse required and heading change achieved for all phases except the atmospheric maneuvering (i.e., deorbit, circularize and pullout, exit and orbital reestablishment), including offsetting the thrust at δ_{opt}, were compiled. The ratio of these two quantities $(\Delta\psi/\Delta V)$ for each entry condition was computed and plotted in Figure 19. Note again the advantage of high L/D vehicles. The optimum entry angle for maximum heading change efficiency is obtained from this figure. The locus of these points is presented in Figure 20. This optimum maneuver line has been indicated by a broken line on all preceding performance curves.

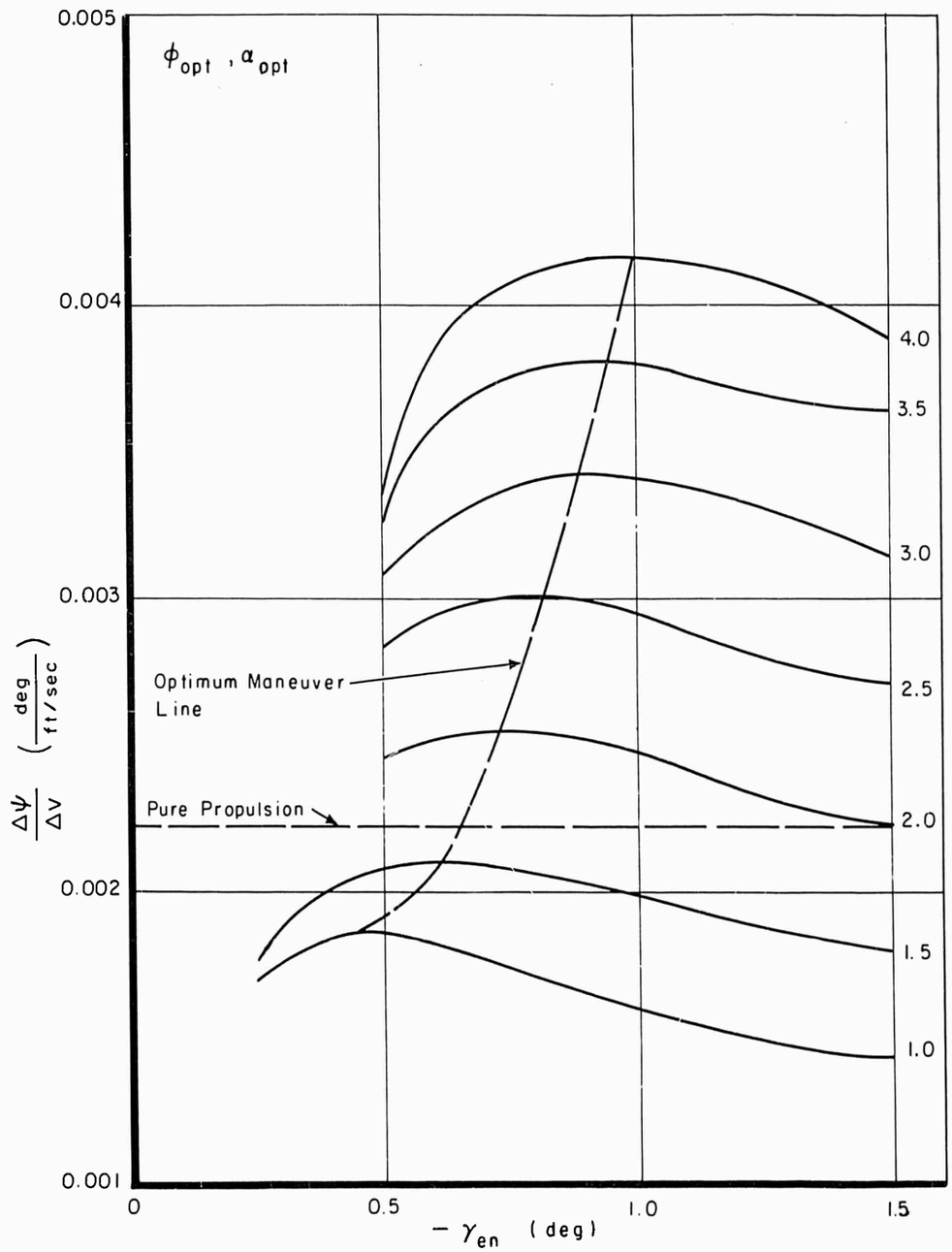

Figure 19. Heading Change Efficiency for Deorbit, Pullout, Exit and Reestablishment Including Thrust Offset for Various L/D Values

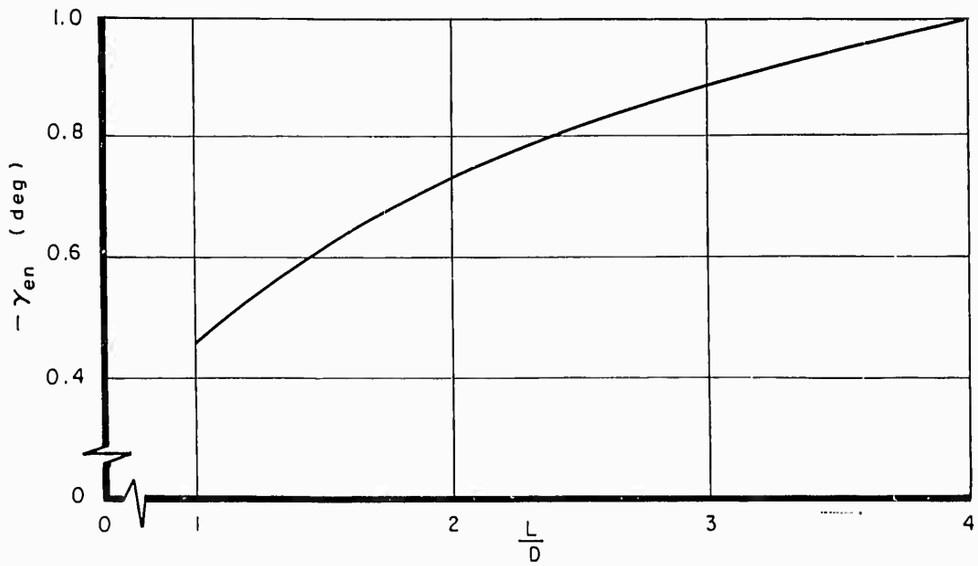

Figure 20. Optimum Entry Angle Versus L/D

Up to this point we have computed heading change ($\Delta\psi$) and not orbital inclination change (Δi). In general, change of heading produces part inclination change and part orbital node change, the ratio depending on the vehicle's location with respect to the equator. Exactly on the equator heading change produces only inclination change while 90° from the equator only node change is achieved. From the consideration of the interaction of the various orbital parameters, it becomes inefficient to perform heading change for extended time periods as shown in Figure 21. For example, 90 percent efficiency results in a maximum turning time of approximately 21 minutes. Times in excess of this result in substantial decreases in turning efficiency, as seen in Figure 21. Consequently, it is necessary to obtain an expression for the time spent in the atmosphere, and then the total time consumed by a given plane change. The time for the turn was computed from an expression for the thrusting, banked turn derived in Appendix III. Since the reentry and exit times can be obtained directly from the computer, they may be added to those calculated by Equation (III-16) and the result is shown in Figure 22. For heading changes greater than those shown in Figure 22, it is necessary to penetrate more deeply into the atmosphere which decreases the turning time, but also decreases the efficiency (Figs. 6 and 19). Since the specific purpose of this report is to define the most efficient maneuver, the above circumstances have not been considered in detail.

One now reaches the point where it is possible to ascertain whether employment of aerodynamic maneuvering and its attendant complexity is really worthwhile. Figure 23 shows the total velocity required to accomplish a given plane change under fully optimized conditions. It is readily apparent that the savings over pure propulsion are substantial. In the extreme, 2300 ft/sec of ΔV allow an L/D = 4 vehicle to attain approximately 300 percent more plane change than for pure propulsion in orbit. Without question, this is a substantial saving.

Figure 24 shows the total time required to perform a given plane change under optimum conditions. While the times are much longer than for pure propulsion, requiring nearly one full orbit for 17° of plane change, this is a small price to pay for the propellant savings attained.

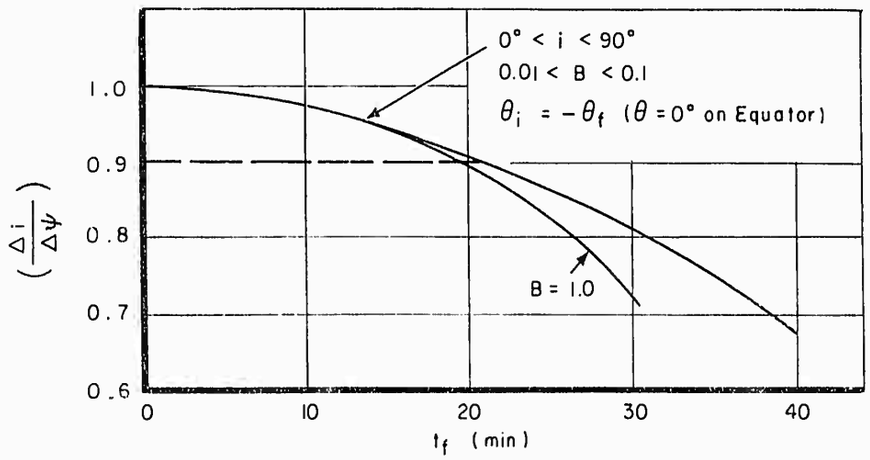

Figure 21. Orbital Inclination Change Efficiency Versus Time

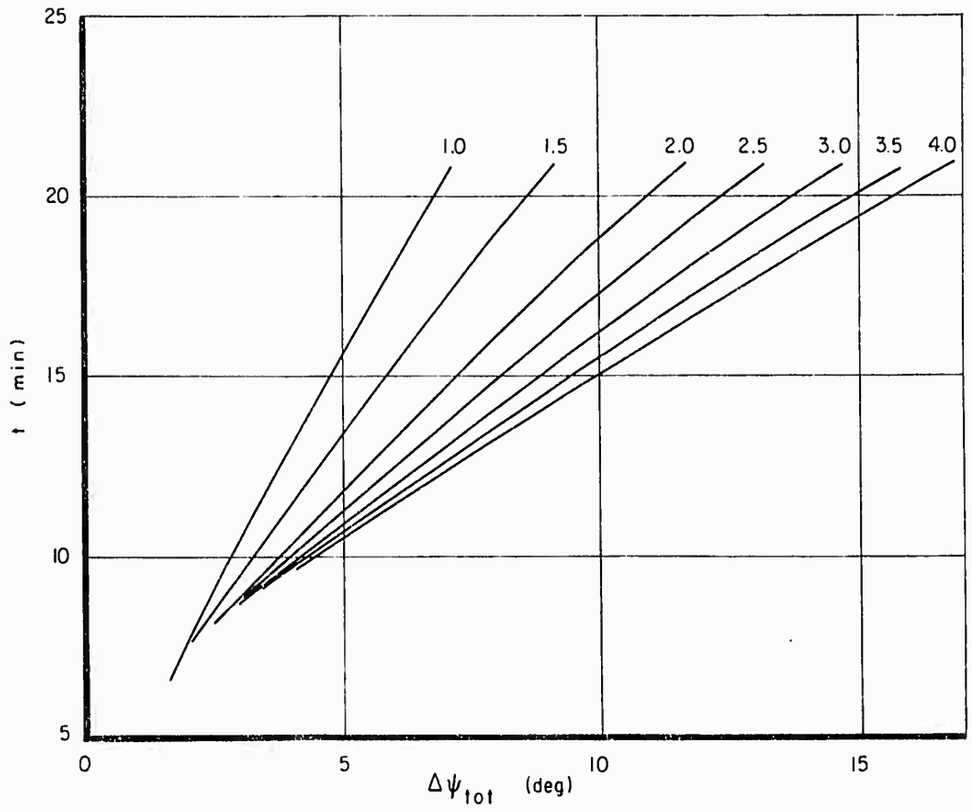

Figure 22. Optimum Turning Time in the Atmosphere for Various L/D Values

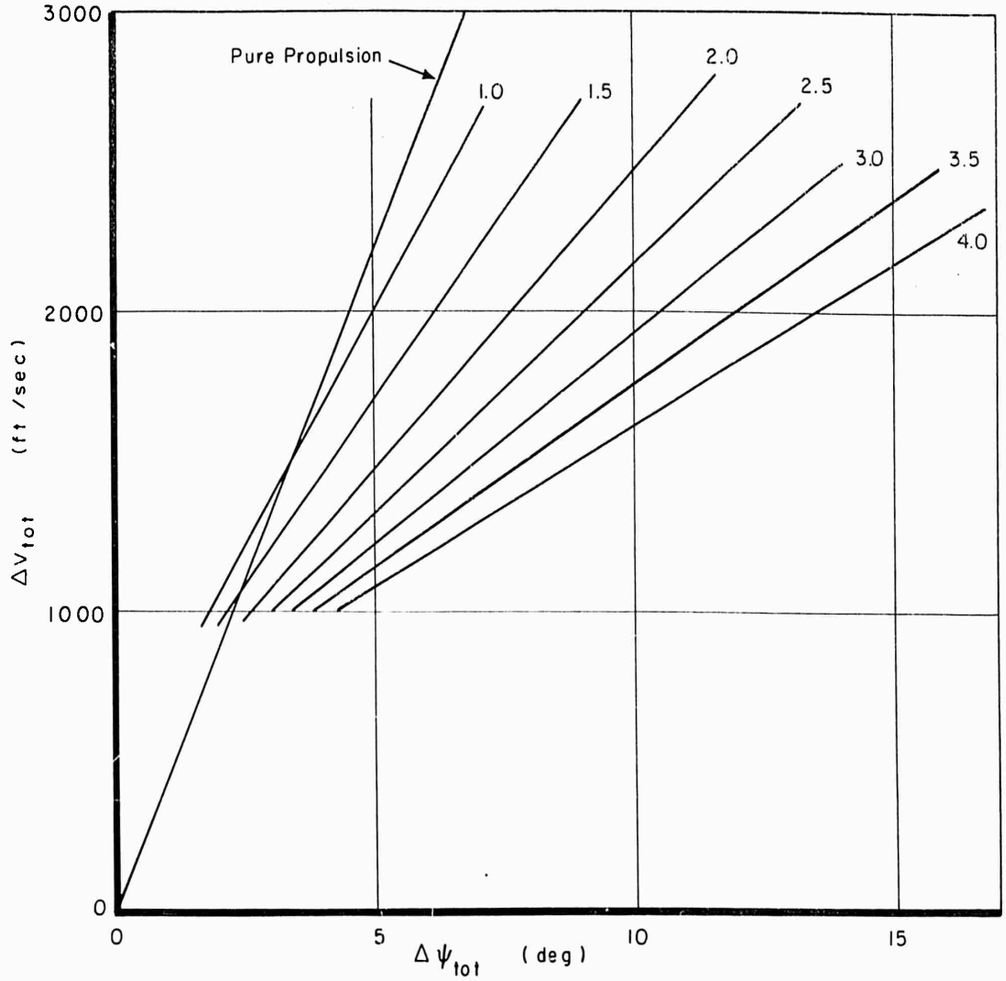

Figure 23. Total Velocity Required for a Given Heading Change for Various L/D Values

Although structural limitations have not been considered, it is interesting to note what demands are made on the structure by this method. Figure 25 depicts the peak, equilibrium, stagnation temperature calculated for the various reentry conditions utilizing the expression (Ref. 5)

$$\left(\frac{T}{1000}\right) = \left[\frac{21}{0.481}\sqrt{\rho_\infty}\left(\frac{V}{1000}\right)^3\right]^{0.25} \tag{37}$$

where a nose radius of one foot and an emissivity of unity have been assumed. Note that for the L/D = 4 optimum maneuver, a peak temperature of 4900°F is reached, which is not beyond the forseeable state of the art for nose cap materials.

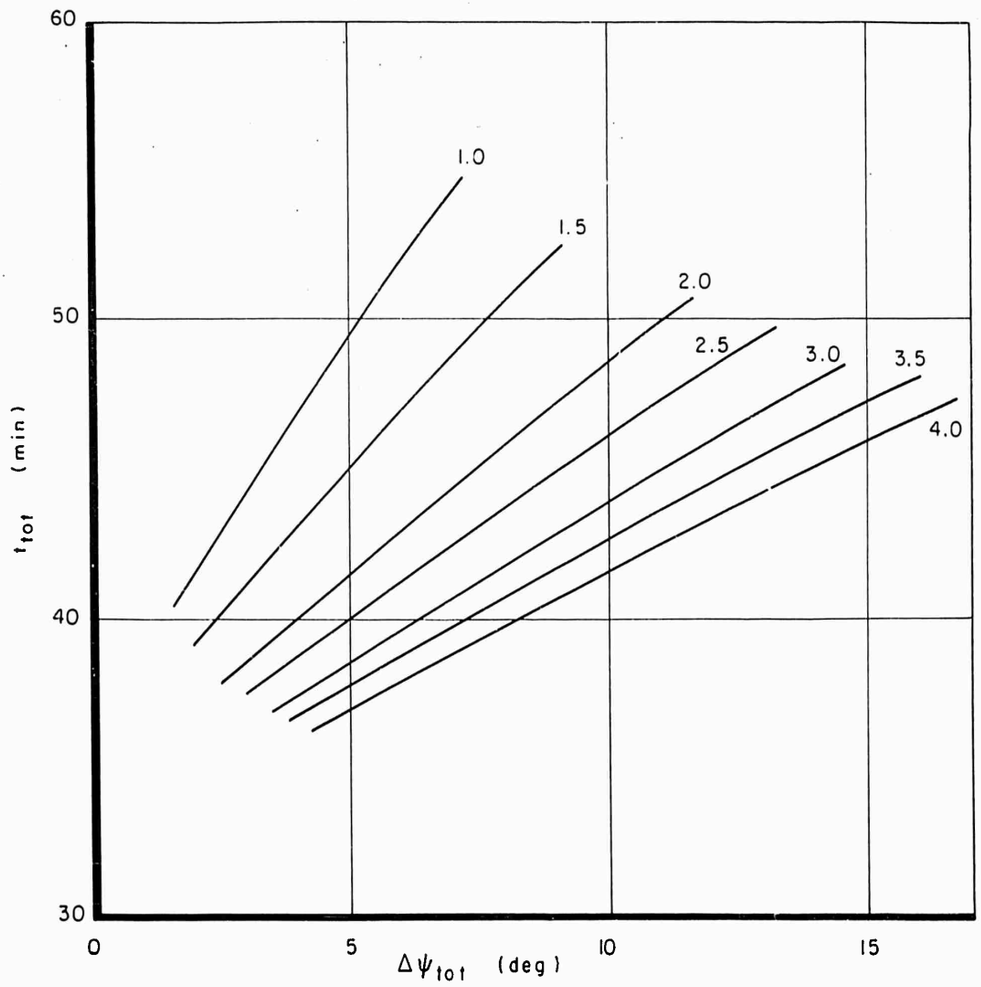

Figure 24. Total Time to Perform a Given Heading Change for Various L/D Values

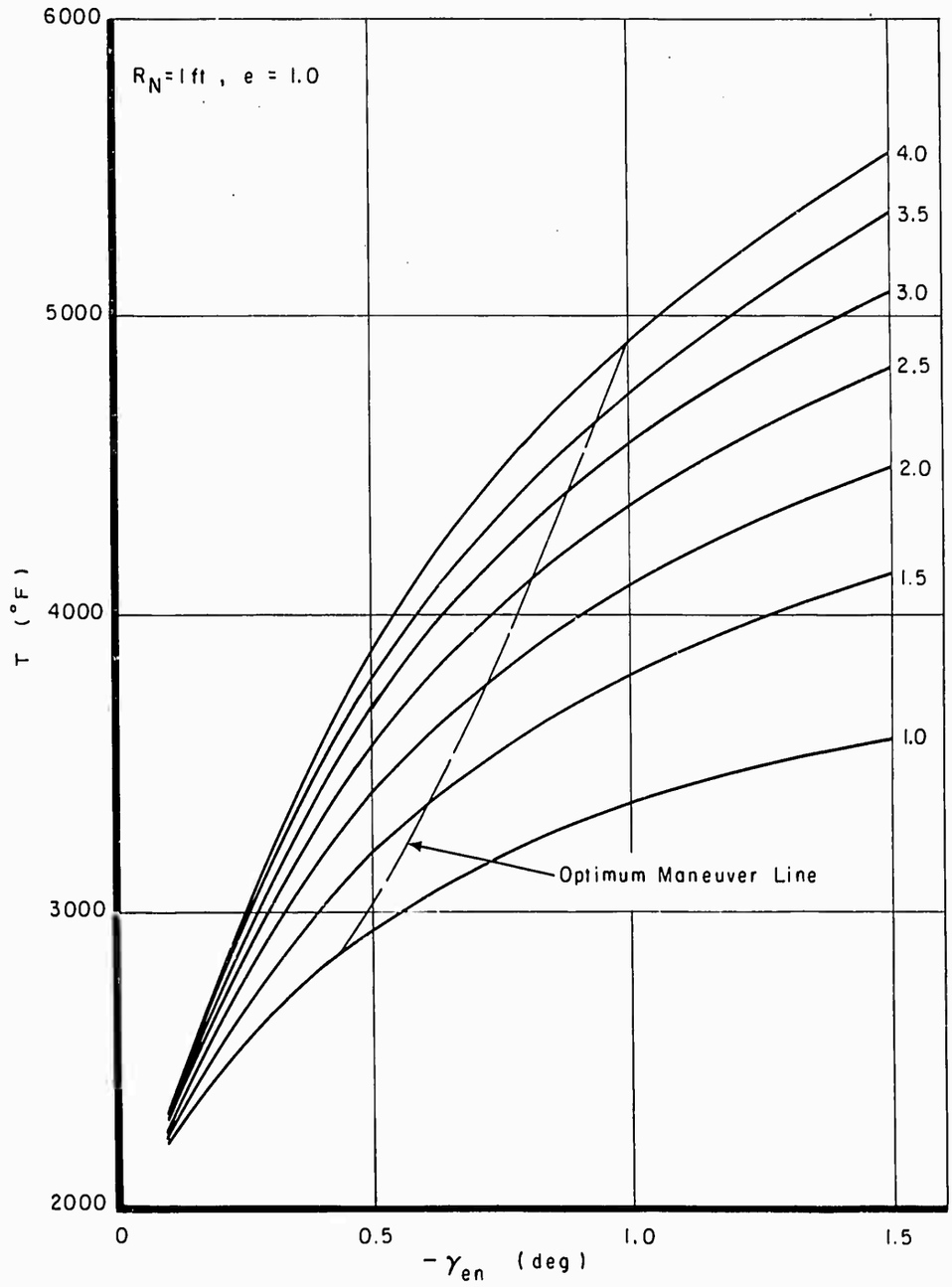

Figure 25. Maximum Nose Stagnation Temperature for Various L/D Values

IV. CONCLUSIONS

A method for accomplishing orbital plane change utilizing atmospheric maneuvering with propulsion augmentation, termed the "synergetic or aeropropulsive method," has been investigated. The performance of vehicles having L/D values from 1 to 4 was compared to a pure propulsion plane change.

From the foregoing analysis the following conclusions are drawn:

(1) The use of aerodynamic maneuvering in performing orbital plane change results in substantial fuel savings over plane change in space especially when one follows the optimum flight path and flight plan described herein and summarized below.

Deorbit is initiated by a retrothrust sufficient in magnitude to enter the atmosphere (by a Hohmann ellipse) at the optimum flight path angle shown in Figure 20. The vehicle is flown at the angle of attack for $(L/D)_{max}$ throughout the entire synergetic maneuver. The optimum bank angle for entry and exit phase is shown in Figure 4. When the vehicle reaches the optimum altitude (Fig. 6) thrust is added to nearly circularize the velocity and the bank angle increased to approximately 90° (Fig. 11). Thrust is then added to maintain constant speed and the lift vector used to change the heading in the "synergetic" turn. After the desired heading change has been accomplished, a velocity impulse (Fig. 15) is added to return to the original orbit, again on a Hohmann ellipse. Finally, velocity is added for recircularization. The velocity impulses added while in the atmosphere are offset at an angle from the original vector to produce higher turning efficiencies (Fig. 16).

(2) Increasing the L/D value of a vehicle substantially improves its plane change efficiency, thus producing greater plane change for each pound of fuel expended. Specifically for an L/D of 4 performance over pure propulsion in orbit was improved by approximately a factor of 3.

(3) Although maneuver time is considerably longer than for pure propulsion, it does not become a constraining factor unless plane changes greater than 17° are desired. In this case, it would be necessary to perform the plane change in stages, with perhaps a half orbit being required between stages, if the efficiency of the method is to be maintained.

(4) Although the temperatures inherent in the optimum procedures are high they are within the foreseeable state of the art for advanced materials.

(5) Unless time is at a premium, or high fuel consumption can be easily tolerated, the application of aerodynamic maneuvering to orbital plane change appears worthy of consideration for future space missions.

APPENDIX I

DERIVATION OF AERODYNAMICS

The aerodynamics used in this report are based on the work of Chapman (Ref. 4). Assuming Newtonian hypersonic flow, the L/D of a vehicle may be written

$$\frac{L}{D} = \frac{\sin^2\alpha \cos\alpha}{b + \sin^3\alpha} \tag{I-1}$$

where

$$b = \frac{C_{D_o}}{C_{D_{mox}} - C_{D_o}} . \tag{I-2}$$

C_{D_o} = the drog coefficient ot $\alpha = 0$

$C_{D_{max}}$ = the drog coefficient ot $\alpha = 90°$.

From this basic definition, several quantities may be obtained. First, it is desired to know the variation of $(L/D)_{max}$ with α_{opt} under the assumed conditions. At α_{opt} $d(L/D)/d\alpha = 0$ and hence, from Equation (I-1)

$$\frac{d\left(\frac{L}{D}\right)}{\left(\frac{L}{D}\right) d\alpha} = 2\cot\alpha - \tan\alpha - \frac{3\sin^2\alpha \cos\alpha}{(b + \sin^3\alpha)} . \tag{I-3}$$

Setting Equation (I-3) equal to zero, an equation for α_{opt} is obtained,

$$b = \frac{\sin\alpha_{opt}}{2\cot^2\alpha_{opt} - 1} . \tag{I-4}$$

Then $(L/D)_{max}$ is defined by

$$\left(\frac{L}{D}\right)_{mox} = \frac{1}{3}\left[2\cot\alpha_{opt} - \tan\alpha_{opt}\right] . \tag{I-5}$$

The value of $(L/D)_{max}$ calculated by Equation (I-5) is shown in Figure I-1. The value of b corresponding to each of these values is obtained from Equation (I-4).

To obtain the C_L and C_D values for each of the $(L/D)_{max}$ values, from the reference

$$C_D = C_{D_o} + \left(C_{D_{mox}} - C_{D_o}\right)\sin^3\alpha \tag{I-6}$$

which, using Equation (I-2) becomes

$$C_D = \left(C_{D_{mox}} - C_{D_o}\right)\left[b + \sin^3\alpha\right] . \tag{I-7}$$

Also, from Equation (I-1), combined with Equation (I-7)

$$C_L = \left(C_{D_{max}} - C_{D_o} \right) \sin^2\alpha \cos\alpha \qquad \text{(I-8)}$$

From the assumption of Newtonian flow,

$$\left(C_{D_{max}} - C_{D_o} \right) = 2 . \qquad \text{(I-9)}$$

Hence

$$C_D = 2 \left[b + \sin^3\alpha \right] \qquad \text{(I-10)}$$

and

$$C_L = 2 \sin^2\alpha \cos\alpha . \qquad \text{(I-11)}$$

Using the value of b and α_{opt} from Equations (I-4) and (I-5), the values of C_L and C_D at $(L/D)_{max}$ are obtained from Equations (I-10) and (I-11). These values are tabulated in Table I-1 with the angle of attack at which they occur.

Figure I-2 has been placed in the report merely for the convenience of the reader. It defines the drag on a vehicle having the L/D value shown when flying at the indicated altitude and at local circular speed over the equator.

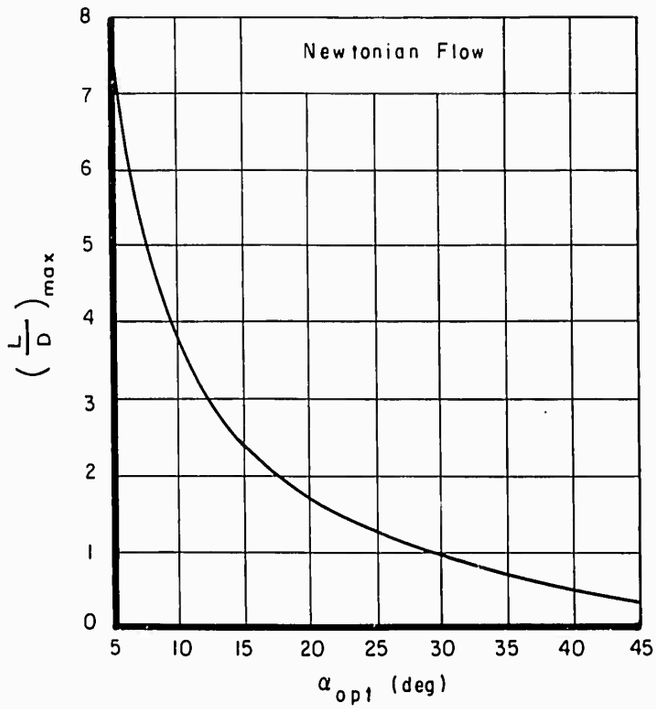

Figure I-1. $(L/D)_{max}$ Versus Angle of Attack

TABLE I-1

VEHICLE CHARACTERISTICS AT $(L/D)_{max}$

$(\frac{L}{D})_{max}$	α_{opt} (degrees)	$C_{L_{opt}}$	$C_{D_{opt}}$	b
0.33	45	0.707107	2.12132	0.707107
0.5	40.4	0.639783	1.279566	0.367534
1.0	29.25	0.41662	0.41662	0.09165
1.5	22.17	0.26374	0.17583	0.03418
2.0	17.51	0.17208	0.08624	0.01593
2.5	14.35	0.11902	0.04761	0.00858
3.0	12.2	0.0873	0.0291	0.0051125
3.5	10.6	0.06652	0.019006	0.032785
4.0	9.35	0.05209	0.013022	0.0022228

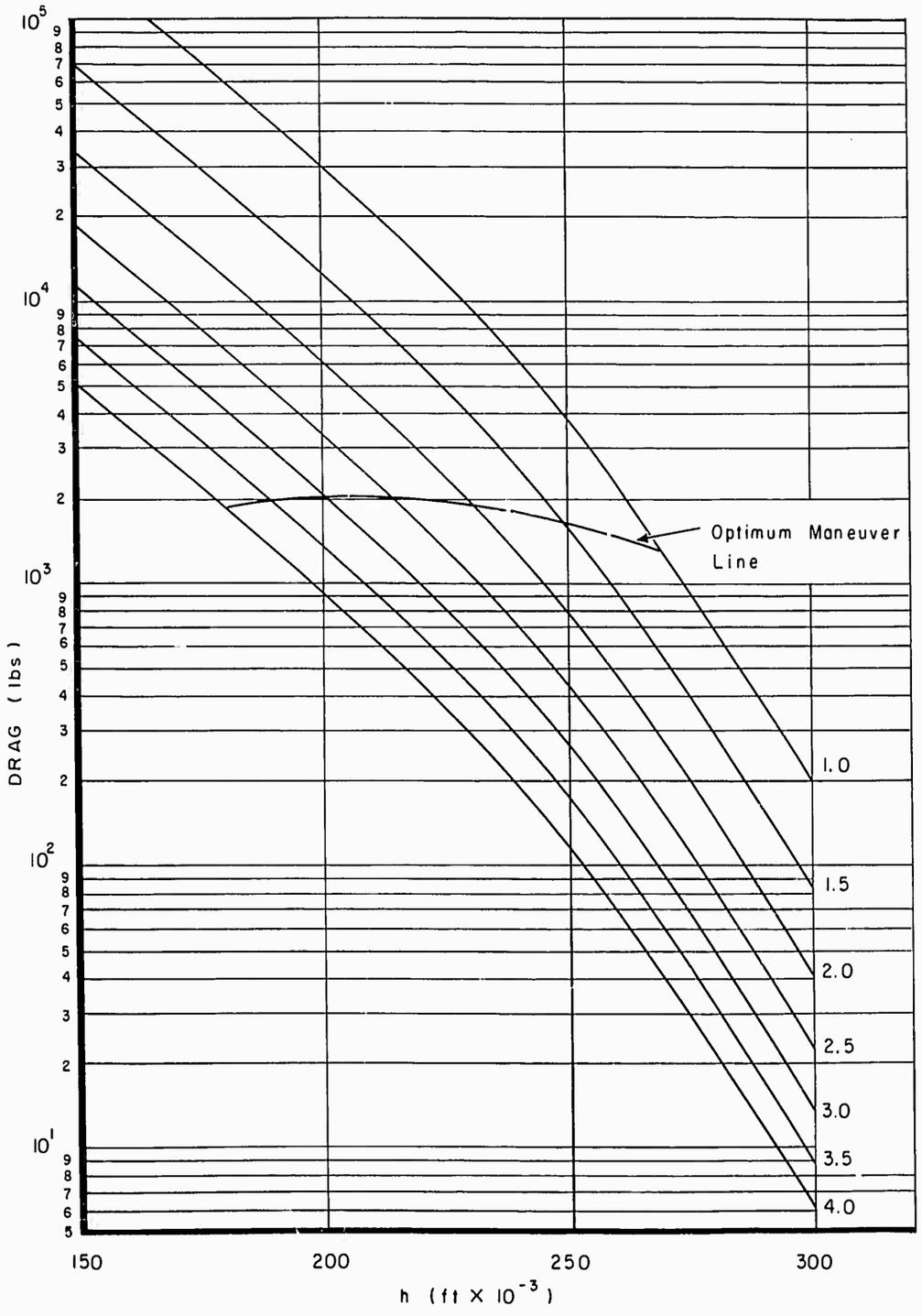

Figure I-2. Drag Variation with Altitude at Circular Velocity for Various L/D Values

APPENDIX II

PARAMETRIC STUDY OF VEHICLE REFERENCE AREA AND MASS

For all of the analyses, a constant reference area and initial mass have been assumed. This assumption is justified from Figures II-1 and II-2 which show, for two bank angles, the effect of mass and reference area variation on the pullout velocity. This parameter is chosen because it is directly related to the energy requirements which are under consideration. It is seen that the effect of the variation of these parameters over the entire range of entry angles is small enough to be neglected. Thus an average value is chosen and held constant throughout the analysis.

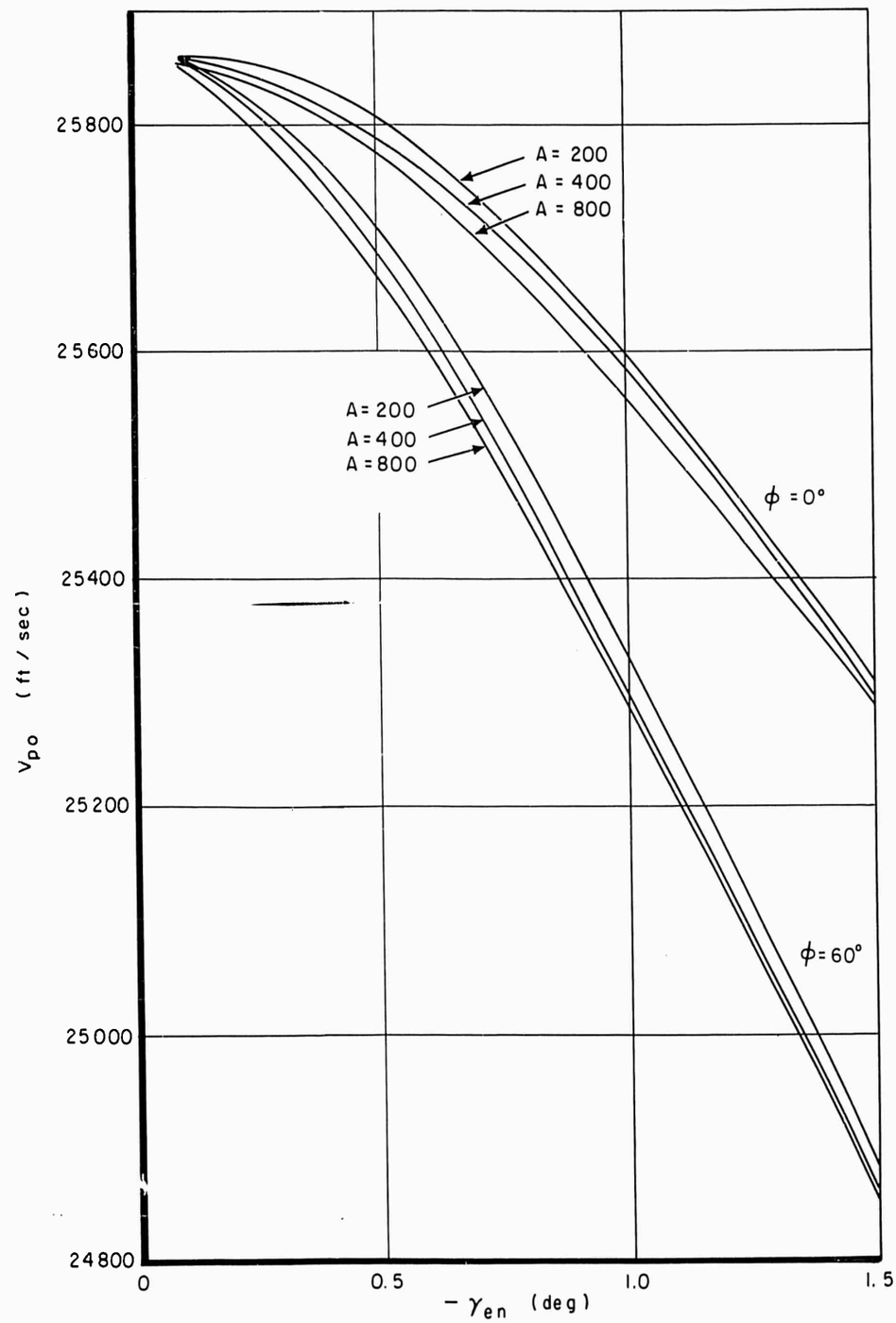

Figure II-1. Effect of Area Variation on Pullout Velocity

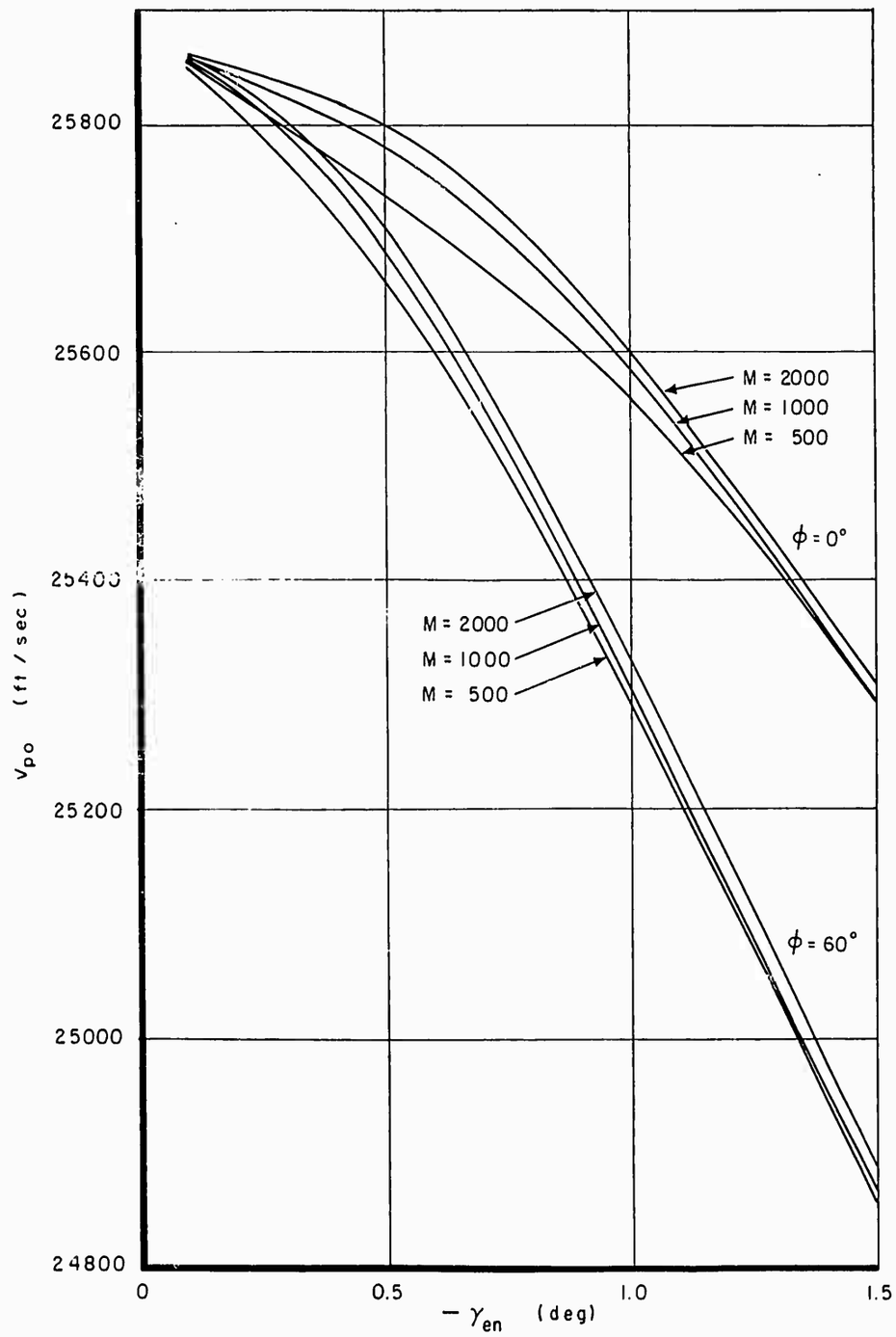

Figure II-2. Effect of Mass Variation on Pullout Velocity

APPENDIX III

TIME REQUIRED TO PERFORM A PLANE CHANGE

Another parameter to be considered in this evaluation is the time required to perform a given plane change utilizing the synergetic method. To obtain the total elapsed time, it is necessary to evaluate each phase independently and to sum the results. For the deorbit and return to orbit phases the equations of classical celestial mechanics may be used to obtain the required time. From the basic equations of motion, it can be shown that the angle swept by a radius vector may be written

$$\tan\theta = \frac{V \sin\gamma}{\frac{\ell_1}{r} - \frac{\mu}{\ell_1}} \tag{III-1}$$

where all values are instantaneous and θ is measured from the orbit perigee. By using basic definitions, Equation (III-1) may be written

$$\tan\theta = \frac{V^2 \sin\gamma \cos\gamma}{V^2 \cos^2\gamma - V_c^2} \, . \tag{III-2}$$

If Equation (III-2) is chosen to represent the deorbit ellipse, following the firing of the retrograde impulse while in a given circular orbit, then the angle swept from retrofire to reentry may be rewritten, in terms of the reentry and original orbit parameters as

$$\tan\theta_{en} = \frac{\left(\frac{V_{en}}{V_{c_1}}\right)^2 \sin\gamma_{en} \cos\gamma_{en}}{\left(\frac{V_{en}}{V_{c_1}} \cos\gamma_{en}\right)^2 - \frac{r_1}{r_{en}}} \, . \tag{III-3}$$

The eccentricity of the reentry orbit can be obtained from the following equation expressed in terms of the radii at the apogee and perigee:

$$\epsilon = 1 - \frac{2 r_p}{r_A + r_p} \, . \tag{III-4}$$

Using the definition of the semi-major axis of an ellipse,

$$2a = r_p + r_A \tag{III-5}$$

the relation

$$\frac{\mu}{a} = \frac{2\mu}{r_A} - V_A^2 \tag{III-6}$$

and the definition of circular velocity

$$V_c^2 = \frac{\mu}{r} \, . \tag{III-7}$$

Equation (III-4) may be written, after considerable manipulation as

$$\epsilon = 1 - \frac{V_A^2}{V_{c_A}^2} \quad . \tag{III-8}$$

To obtain the time required for the vehicle to start reentry after the retrograde impulse, Kepler's law of equal areas swept by a radius vector in equal times yields

$$\frac{dA}{dt} = \text{Constant} = \frac{\ell^*}{2} \tag{III-9}$$

or

$$dt = \frac{r^2}{\ell^*}\, d\theta \tag{III-10}$$

where θ is the angle swept.

Since, in general, the radius r is given by

$$r = \frac{\frac{\ell^{*2}}{\mu}}{1 + \epsilon \cos\theta} \quad , \tag{III-11}$$

Equation (III-10) may be integrated for an ellipse ($0 < \epsilon < 1$) to yield

$$t_2 - t_1 = \frac{\ell^3}{\mu^2}\left\{\frac{\sin\theta}{(\epsilon^2-1)(1+\epsilon\cos\theta)} - \frac{1}{\epsilon^2-1}\left[\frac{2}{\sqrt{1-\epsilon^2}}\tan^{-1}\frac{(1-\epsilon)}{\sqrt{1-\epsilon^2}}\tan\frac{\theta}{2}\right]\right\}\Bigg|_{\theta_1}^{\theta_2} \tag{III-12}$$

By virtue of the fact that on a circular orbit the values of a parameter at all points are the same, the point of retrofire will be taken as the apogee which, in fact, it is for the transfer ellipse. Thus $\theta_1 = \pi$ by definition and Equation (III-12) becomes, since $t_1 = 0$, after some manipulation

$$t_{en} = \frac{r_{en} V_{en} \cos\gamma_{en}}{V_{c_A}^2 (1+\epsilon_2)}\left\{\frac{2}{\sqrt{1-\epsilon_2^2}}\tan^{-1}\left[\sqrt{\frac{1-\epsilon_2}{1+\epsilon_2}}\tan\frac{\theta_{en}}{2}\right] - \tan\gamma_{en}\right\}$$

$$- \frac{\pi r_A}{V_{c_A}(1+\epsilon_2)^{3/2}} \tag{III-13}$$

where

θ_{en} is defined by Equation (III-3) and ϵ_2 by Equation (III-8).

By treating the exit maneuver as the reverse of reentry, Equations (III-3), (III-8) and (III-13) may be used to calculate the exit conditions and the apogee values of the parameters for the completion of the maneuver. The time required to enter the atmosphere and pullout and exit the atmosphere are obtained directly from the computer runs.

The time required to perform the atmospheric maneuver may be obtained from Equations (26), (24), (15), (19) and (23). Integration of Equation (23) determines the mass ratio

$$\ell n \frac{m_2}{m_1} = - \frac{V \Delta \psi}{V_{ex} \sin \phi \sqrt{\left(\frac{L}{D}\right)^2 + 1}} \quad . \tag{III-14}$$

Assuming $\dot{m}$ is constant, then

$$\Delta t_{man} = \frac{\Delta m}{\dot{m}} = \frac{m_2 - m_1}{\dot{m}} \quad . \tag{III-15}$$

Thus, utilizing Equations (III-15), (III-14), (15) and (19), the maneuver time may be written as

$$\Delta t_{man} = \frac{m_1 V_{ex} \cos \Lambda}{D} \left[1 - \exp \left(- \frac{V \Delta \psi}{V_{ex} \sin \phi \sqrt{\left(\frac{L}{D}\right)^2 + 1}} \right) \right] . \tag{III-16}$$

The times calculated by Equation (III-16), added to the time required to enter and exit the atmosphere are shown in Figure 13. A useful engineering approximation for small angles is

$$\Delta t_{man} = \frac{V_c}{g} \left(\frac{W}{L}\right) \Delta \psi = \frac{(2.35)_{minutes}}{\frac{L}{W}} \left(\frac{\Delta \psi^\circ}{10^\circ}\right) . \tag{III-17}$$

REFERENCES

1. F. S. Nyland, The Synergetic Plane Change for Orbiting Spacecraft, Memorandum RM3231-PR, The Rand Corporation, August, 1962.

2. Walter Hohmann, The Attainability of Heavenly Bodies, NASA Technical Translation, TT-F-44, November, 1960.

3. Dr. F. R. Moulton, An Introduction to Celestial Mechanics, The Macmillan Company, New York, 1959.

4. Dean R. Chapman, An Analysis of the Corridor and Guidance Requirements for Supercircular Entry into Planetary Atmospheres, NASA Technical Report, R-55, 1959.

5. Dr. Wilbur L. Hankey, Jr., Richard D. Neumann, and Evard H. Flinn, Design Procedures for Computing Aerodynamic Heating at Hypersonic Speeds, WADC Technical Report 59-610, Wright-Patterson Air Force Base, Ohio, June, 1960.

ACKNOWLEDGMENT

The authors wish to gratefully acknowledge the following individuals for their assistance and cooperation throughout this study: Messrs William Hopkins, James Caslin, Kenneth Cunningham and Mrs. Leotta Joanne Conniff for guidance in and preparation of the computer parametric studies; and Mr. Kenneth Cunningham and Miss Kathryn Beighle for the accomplishment of the manuscript.